

# Adaptive Sampling Bi-Fidelity Stochastic Trust Region Method for Derivative-Free Stochastic Optimization

Yunsoo Ha<sup>\*1</sup> and Juliane Mueller<sup>†1</sup>

<sup>1</sup>Computational Science Center, National Renewable Energy Laboratory,  
15013 Denver West Parkway, Golden, 80401, Colorado, USA

## Abstract

Bi-fidelity stochastic optimization is increasingly favored for streamlining optimization processes by employing a cost-effective *low-fidelity* (LF) function, with the goal of optimizing a more expensive *high-fidelity* (HF) function. In this paper, we introduce ASTRO-BFDF, a new adaptive sampling trust region method specifically designed for solving unconstrained bi-fidelity stochastic derivative-free optimization problems. Within ASTRO-BFDF, the LF function serves two purposes: first, to identify better iterates for the HF function when a high correlation between them is indicated by the optimization process, and second, to reduce the variance of the HF function estimates by Bi-fidelity Monte Carlo (BFMC). In particular, the sample sizes are *dynamically* determined with the option of employing either crude Monte Carlo or BFMC, while balancing optimization error and sampling error. We demonstrate that the iterates generated by ASTRO-BFDF converge to the first-order stationary point almost surely. Additionally, we numerically demonstrate the superiority of our proposed algorithm by testing it on synthetic problems and simulation optimization problems with discrete event simulations.

## 1 Introduction

We consider the simulation optimization problem

$$\min_{\mathbf{x} \in \Re^d} f^h(\mathbf{x}) := \mathbb{E}[F^h(\mathbf{x}, \xi)] = \int_{\Xi} F^h(\mathbf{x}, \xi) P(d\xi), \quad (1)$$

where  $f^h : \Re^d \rightarrow \Re$  is nonconvex and bounded from below, and  $F^h : \Re^d \times \Xi \rightarrow \Re$  is a random function with the random element  $\xi$  having distribution  $P$  on the measurable space  $(\Xi, \mathcal{F})$ . So,  $\xi : \Omega \rightarrow \Xi$  is an  $\mathcal{F}$ -measurable function. In addition, we consider *zeroth-order stochastic oracles*, where the derivative information is not directly available from the Monte Carlo simulation.

The function  $F^h(\mathbf{x}, \xi)$  can be generated through the invocation of a stochastic simulation oracle. Furthermore, we assume that there exists an additional stochastic simulation oracle capable of approximating  $F^h(\mathbf{x}, \xi)$  at a lower cost than the original simulation oracle. This cost-effective oracle, termed the low-fidelity (LF) simulation, generates  $F^l : \Re^d \times \Xi \rightarrow \Re$  with  $f^l(\mathbf{x}) := \mathbb{E}[F^l(\mathbf{x}, \xi)]$ .

---

<sup>\*</sup>yunsoo.ha@nrel.gov

<sup>†</sup>juliane.mueller@nrel.gov

## 1.1 Bi-fidelity Derivative-free Stochastic Optimization

The iterative algorithms designed to solve problem (1) typically produce a random sequence  $\{\mathbf{X}_k, k \geq 1\}$ . In the context of SO, these algorithms generate the sequence by determining both the direction and the step size. Given that direct gradient information is not available from the simulation oracle, we rely on approximation techniques like a finite difference method [1], interpolation/regression models [2, 3, 4], and Gaussian smoothing [5] to determine the direction. These approximation methods are based on function estimates, which are obtained by repeatedly invoking the stochastic simulation oracle, as shown below:

$$\bar{F}^h(\mathbf{x}, n) = \frac{1}{n} \sum_{i=1}^n F^h(\mathbf{x}, \xi_i), \quad (2)$$

with a variance estimate  $(\hat{\sigma}^h)^2(\mathbf{x}, n) := n^{-1} \sum_{i=1}^n (F^h(\mathbf{x}, \xi_i) - \bar{F}^h(\mathbf{x}, n))^2$ . To obtain the convergence results in some probabilistic senses, the algorithms must have sufficiently large sample sizes for each design point during the optimization process. Therefore, it is a logical step to aim for reducing the total number of simulation replications during the optimization process while still achieving convergence, as this is typically the main source of computational load. In line with these efforts, one strategy involves leveraging a LF simulation oracle  $F^l(\cdot, \xi)$ , which is less costly than the original high-fidelity (HF) simulation oracle  $F^h(\cdot, \xi)$ , whenever possible throughout the optimization process. This particular method of optimization falls under the category of bi-fidelity stochastic optimization [6, 7, 8, 9].

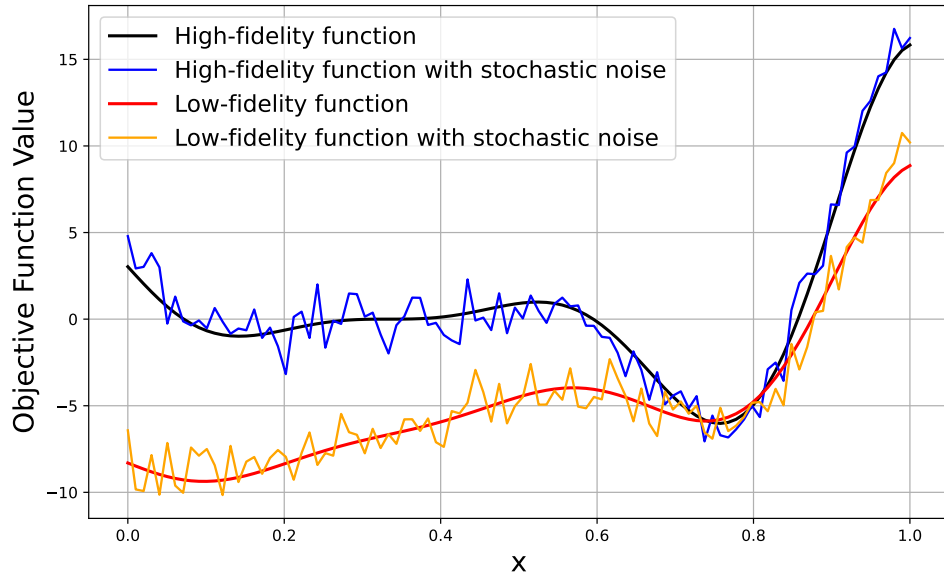


FIGURE 1: An illustration of bi-fidelity functions. The black and red curves represent the true objective functions of the HF and LF versions, respectively. Meanwhile, the blue and orange curves illustrate a *single sample path* of the stochastic objective functions for the HF and LF versions, respectively.

It is reasonable to expect that employing a LF simulation oracle can expedite convergence by providing more information at a lower cost. For example, the iterative algorithm can yield

a near-optimal solution of the HF function, even though the LF function is solely utilized, as illustrated in Figure 1. However, the specifics of how and when to utilize the LF simulation oracle have remained elusive, prompting us to pose two overarching questions.

- Q1. When is it appropriate to utilize the LF simulation oracle, and when should it not be used during optimization?
- Q2. What number of sample sizes for HF and LF simulation oracles are necessary to attain sufficiently accurate function estimates for optimization?

In this paper, we propose a *sample-efficient* solver for bi-fidelity stochastic optimization, aiming to address questions Q1 and Q2 specifically. We begin by introducing relevant existing sampling methods that have been used for sample-efficient uncertainty quantification, regardless of their purpose for optimization.

## 1.2 Adaptive Sampling

In derivative-free stochastic optimization, ensuring the precision of gradient approximations relies on acquiring accurate estimates of function values, a task typically accomplished by averaging a significant number of samples. Given the large computational cost associated with each stochastic simulation oracle call, the necessity for numerous calls to achieve the required precision poses a challenge in finding a sufficiently viable solution to the optimization problem within a reasonable timeframe. This prompts the research question: “How can we ascertain the appropriate sample sizes for each design point visited by the optimization algorithm?”

Typically, a fixed sample size may not ensure a convergence of  $\{\mathbf{X}_k\}$  because when  $\mathbf{X}_k$  is close enough to the stationary point, the stochastic error may exceed the gap in function values between the current iterate and the next iterate. Therefore, many stochastic algorithms [2, 10] typically utilize a deterministic sample size, which increases based on optimality measures such as gradient approximations. Nonetheless, relying solely on deterministic sample sizes could pose practical challenges, as the variance of each design point is often unknown. Therefore, in order to intelligently ascertain an appropriate sample size, an Adaptive Sampling (AS) strategy has been implemented within the iterative algorithms [10, 11]. The AS strategy dynamically decides the sample size by striking a balance between the estimation error at each point and the optimality measure. With the estimation error continuously updated through replicating function evaluations, the AS strategy yields a random sample size based on the observations generated at the design point of interest.

The AS strategy has been proposed based on a crude Monte Carlo (CMC) estimation (2) for situations where only one simulation oracle is available [10, 11, 12]. However, when multiple simulation oracles of different fidelities are available, a different Monte Carlo method, referred to as multi-fidelity Monte Carlo (MFMC) [13], can be used to reduce the variance of the estimator, which will be introduced in the next section.

## 1.3 Bi-fidelity Monte Carlo

In the domain of uncertainty quantification, a function estimate for a single design point is typically derived through a crude Monte Carlo (CMC) estimation (2). However, due to the slow convergence rate of CMC, which grows only as the square root of the sample sizes, it may be impractical to obtain sufficiently accurate function estimates within a reasonable timeframe, particularly when dealing with costly stochastic simulation oracles. Hence, when multi-fidelity simulation oracles are

available, the HF function estimate is obtained using both LF and HF simulation oracles hoping that it can reduce the variance of the HF function estimate [13]. A bi-fidelity Monte Carlo (BFMC) is then  $\bar{F}^{\text{bf}}(\mathbf{x}, n, v, c) = \bar{F}^h(\mathbf{x}, n) - c(\bar{F}^l(\mathbf{x}, n) - \bar{F}^l(\mathbf{x}, v))$  for any  $c \in \mathfrak{R}$ , which is an unbiased estimator of the expectation of the HF function. Here, the independence or dependence between  $\bar{F}^l(\mathbf{x}, v)$  and  $\bar{F}^h(\mathbf{x}, n)$ , as well as  $\bar{F}^l(\mathbf{x}, n)$ , hinges on how the random variable  $\xi$  is managed. For instance, consider (3), which employs  $v^{-1} \sum_{i=1}^v F^l(\mathbf{x}, \xi_i)$  for  $\bar{F}^l(\mathbf{x}, v)$ :

$$\bar{F}^{\text{bf}}(\mathbf{x}, n, v, c) = \frac{1}{n} \sum_{i=1}^n F^h(\mathbf{x}, \xi_i) - c \left( \frac{1}{n} \sum_{i=1}^n F^l(\mathbf{x}, \xi_i) - \frac{1}{v} \sum_{i=1}^v F^l(\mathbf{x}, \xi_i) \right). \quad (3)$$

Then the variance of  $\bar{F}^{\text{bf}}(\mathbf{x}, n, v, c)$  becomes

$$\begin{aligned} & c^2(\text{Var}(\bar{F}^l(\mathbf{x}, n)) + \text{Var}(\bar{F}^l(\mathbf{x}, v))) - 2c\text{Cov}(\bar{F}^h(\mathbf{x}, n), \bar{F}^l(\mathbf{x}, n)) \\ & + 2c\text{Cov}(\bar{F}^h(\mathbf{x}, n), \bar{F}^l(\mathbf{x}, v)) - 2c^2\text{Cov}(\bar{F}^l(\mathbf{x}, n), \bar{F}^l(\mathbf{x}, v)) + \text{Var}(\bar{F}^h(\mathbf{x}, n)). \end{aligned} \quad (4)$$

Therefore, variance reduction becomes feasible with appropriate covariances and variances for certain values of  $n$ ,  $v$ , and  $c$ .

In our proposed algorithm, we have developed an innovative AS strategy, referred as bi-fidelity Adaptive Sampling (BAS), that leverages both LF and HF oracles. Our approach dynamically employs BFMC and CMC, guided by estimates of covariances and variances for the functions. While we expect that BAS can be deployed within a broad range of iterative solvers, we focus exclusively on stochastic Trust Region (TR) algorithms to solve (1).

#### 1.4 Stochastic Trust Region Algorithms for Derivative-free Stochastic Optimization

The popularity of stochastic TR algorithms has recently surged for addressing (1) due to their robustness, which comes from their ability to self-tune and naturally utilize curvature information in determining step lengths. Stochastic TR algorithms typically entail the following four steps in every iteration  $k$ :

- (a) (model construction) a local model is constructed to approximate the objective function  $f$  by utilizing specific design points and their function estimates within a designated area of confidence, i.e., TR, typically defined as an  $L_2$  region with a radius of  $\Delta_k$  centered around the current iterate  $\mathbf{X}_k$ ;
- (b) (subproblem minimization) a candidate point  $\mathbf{X}_k^s$  is obtained by approximately minimizing the local model within the TR;
- (c) (candidate evaluation) the objective function at  $\mathbf{X}_k^s$  is estimated by querying the oracle, and depending on this evaluation,  $\mathbf{X}_k^s$  is either accepted or rejected; and
- (d) (TR management) if  $\mathbf{X}_k^s$  is accepted, it becomes the subsequent iterate  $\mathbf{X}_{k+1}$ , and the TR radius  $\Delta_k$  is either enlarged or remains unchanged; conversely, if  $\mathbf{X}_k^s$  is rejected,  $\mathbf{X}_k$  retains its position as the next iterate  $\mathbf{X}_{k+1}$ , and  $\Delta_k$  decreases to facilitate the construction of a more accurate local model to approximate the objective function  $f$ .

As described in Section 3.2, our proposed algorithm performs the aforementioned four steps multiple times within a single iteration to address Q1, utilizing both HF and LF simulation oracles.

Specifically, when the correlation between the LF and HF function is expected to be high, which is determined by the optimization history, the local models will be constructed for the LF function. If we fail to find a better solution using the local model for the LF function, the local model will be constructed for the HF function within the same iteration.

## 1.5 Summary of Results and Insight.

In this section, we summarize our contribution and results.

- (a) We propose a novel stochastic TR method with adaptive sampling tailored specifically for stochastic bi-fidelity optimization problems, aptly named ASTRO-BFDF. Addressing Q1, ASTRO-BFDF integrates two separate TRs to handle HF and LF functions, along with a novel concept termed an adaptive correlation constant. This constant dynamically assesses the need for constructing a local model for the LF function, with its value evolving in response to the historical data gathered during the optimization process.
- (b) To provide an answer for Q2, we suggest a new adaptive sampling algorithm utilizing both HF and LF simulation oracles, named BAS. The following three critical decisions are dynamically made in BAS while replicating function evaluations.
  - At a given  $\mathbf{x} \in \mathbb{R}^d$ , is BFMC cheaper than CMC?
  - What are the best sample sizes for the LF and HF simulation oracles and the best coefficient  $c$  for BFMC in (3)?
  - Is an accuracy of the function estimate from BAS sufficient to proceed with the optimization at the current iteration?
- (c) We prove the almost sure convergence, i.e.,  $\lim_{k \rightarrow \infty} \|\nabla f^h(\mathbf{X}_k)\| = 0$  w.p.1, of ASTRO-BFDF. The analysis revolves around two key points. Firstly, when the candidate solution from the local model for the LF function is accepted, it must ensure a sufficient reduction in the HF function. Secondly, the estimates for stochastic errors obtained with BFMC should be sufficiently smaller than the optimality error. Together, these aspects enable the algorithm to find a better solution for the objective function with reduced computational effort.
- (d) The performance of ASTRO-BFDF has been evaluated using test problems from the SimOpt library [14]. We started with synthetic problems, created by adding artificial stochastic noise to deterministic functions. For more realistic numerical experiments, we also tested simulation optimization problems involving discrete event simulation. Our findings not only highlight the superior performance of ASTRO-BFDF but also explore various scenarios in which using the LF function in optimization is beneficial or not.

## 2 Preliminaries

In this section, we provide key definitions, standing assumptions, and some useful results that will be invoked in the convergence analysis of the proposed algorithm.

### 2.1 Notation

We use bold font for vectors;  $\mathbf{x} = (x_1, x_2, \dots, x_d) \in \mathbb{R}^d$  denotes a  $d$ -dimensional vector. Calligraphic fonts represent sets, and sans serif fonts denote matrices. Our default norm  $\|\cdot\|$  is the  $L_2$

norm. The closed ball of radius  $\Delta > 0$  centered at  $\mathbf{x}^0$  is  $\mathcal{B}(\mathbf{x}^0; \Delta) = \{\mathbf{x} \in \mathbb{R}^d : \|\mathbf{x} - \mathbf{x}^0\| \leq \Delta\}$ . For a sequence of sets  $\mathcal{A}_n$ ,  $\mathcal{A}_n$  i.o. denotes  $\limsup_{n \rightarrow \infty} \mathcal{A}_n$ . We write  $f(\mathbf{x}) = \mathcal{O}(g(\mathbf{x}))$  if there are positive constants  $\varepsilon$  and  $m$  such that  $|f(\mathbf{x})| \leq mg(\mathbf{x})$  for all  $\mathbf{x}$  with  $0 < \|\mathbf{x}\| < \varepsilon$ . Capital letters denote random scalars and vectors. For a sequence of random vectors  $\mathbf{X}_k$ ,  $k \in \mathbb{N}$ ,  $\mathbf{X}_k \xrightarrow{w.p.1} \mathbf{X}$  denotes almost sure convergence. “iid” means independent and identically distributed, and “w.p.1” means with probability 1. The superscripts  $h$  and  $l$  indicate that the terminology is related to high-fidelity and low-fidelity simulations, respectively. The terms  $\hat{\sigma}^h(\mathbf{x}, n)$  and  $\hat{\sigma}^l(\mathbf{x}, n)$  are the standard deviation estimates of HF and LF functions at  $\mathbf{x}$  with sample size  $n$ , while  $\hat{\sigma}^{h,l}(\mathbf{x}, n)$  is the covariance estimate between them.

## 2.2 Key Definitions

**Definition 1** (stochastic interpolation models). *Given  $\mathbf{X}_k = \mathbf{X}_k^0 \in \mathbb{R}^d$  and  $\Delta_k^q > 0$ , let  $\Phi(\mathbf{x}) = [\phi_0(\mathbf{x}), \phi_1(\mathbf{x}), \dots, \phi_p(\mathbf{x})]$  be a polynomial basis on  $\mathbb{R}^d$ . With  $p = d(d+3)/2$ ,  $q \in \{h, l\}$  and the design set  $\mathcal{X}_k := \{\mathbf{X}_k^i\}_{i=1}^p \subset \mathcal{B}(\mathbf{X}_k; \Delta_k^q)$ , we find  $\boldsymbol{\nu}_k^q = [\nu_{k,0}^q, \nu_{k,1}^q, \dots, \nu_{k,p}^q]^\top$  such that*

$$\mathbf{M}(\Phi, \mathcal{X}_k) \boldsymbol{\nu}_k = [\bar{F}_k^q(\mathbf{X}_k^0, N(\mathbf{X}_k^0))), \bar{F}_k^q(\mathbf{X}_k^1, N(\mathbf{X}_k^1)), \dots, \bar{F}_k^q(\mathbf{X}_k^p, N(\mathbf{X}_k^p))]^\top, \quad (5)$$

where

$$\mathbf{M}(\Phi, \mathcal{X}_k) = \begin{bmatrix} \phi_1(\mathbf{X}_k^0) & \phi_2(\mathbf{X}_k^0) & \dots & \phi_p(\mathbf{X}_k^0) \\ \phi_1(\mathbf{X}_k^1) & \phi_2(\mathbf{X}_k^1) & \dots & \phi_p(\mathbf{X}_k^1) \\ \vdots & \vdots & \vdots & \vdots \\ \phi_1(\mathbf{X}_k^p) & \phi_2(\mathbf{X}_k^p) & \dots & \phi_p(\mathbf{X}_k^p) \end{bmatrix}.$$

The matrix  $\mathbf{M}(\Phi, \mathcal{X}_k)$  is nonsingular if the set  $\mathcal{X}_k$  is poised in  $\mathcal{B}(\mathbf{X}_k; \Delta_k^q)$ . A set  $\mathcal{X}_k$  is  $\Lambda$ -poised in  $\mathcal{B}(\mathbf{X}_k; \Delta_k^q)$  if  $\Lambda \geq \max_{i=0, \dots, p} \max_{\mathbf{z} \in \mathcal{B}(\mathbf{X}_k; \Delta_k^q)} |l_i(\mathbf{z})|$ , where  $l_i(\mathbf{z})$  are the Lagrange polynomials. If there exists a solution to (5), then the function  $M_k^q : \mathcal{B}(\mathbf{X}_k; \Delta_k^q) \rightarrow \mathbb{R}$ , defined as  $M_k^q(\mathbf{x}) = \sum_{j=0}^p \nu_{k,j}^q \phi_j(\mathbf{x})$  is a stochastic polynomial interpolation of estimated values of  $f^q$  on  $\mathcal{B}(\mathbf{X}_k; \Delta_k^q)$ . In particular, if  $\mathbf{G}_k^q := [\nu_{k,1}^q \ \nu_{k,2}^q \ \dots \ \nu_{k,d}^q]^\top$  and  $\mathbf{H}_k^q$  is a symmetric  $d \times d$  matrix with elements uniquely defined by  $(\nu_{k,d+1}^q, \nu_{k,d+2}^q, \dots, \nu_{k,p}^q)$ , then we can define the stochastic quadratic model  $M_k^q : \mathcal{B}(\mathbf{X}_k; \Delta_k^q) \rightarrow \mathbb{R}$ , as

$$M_k^q(\mathbf{x}) = \nu_{k,0}^q + (\mathbf{x} - \mathbf{X}_k)^\top \mathbf{G}_k^q + \frac{1}{2} (\mathbf{x} - \mathbf{X}_k)^\top \mathbf{H}_k^q (\mathbf{x} - \mathbf{X}_k). \quad (6)$$

**Definition 2** (stochastic fully linear models). *Given  $\mathbf{x} \in \mathbb{R}^d$ ,  $\Delta^q > 0$  and  $q \in \{h, l\}$ , a function  $M^q : \mathcal{B}(\mathbf{x}; \Delta^q) \rightarrow \mathbb{R}$  is a stochastic fully linear model of  $f^q$  on  $\mathcal{B}(\mathbf{x}; \Delta^q)$  if  $\nabla f^q$  is Lipschitz continuous with constant  $\kappa_L$ , and there exist positive constants  $\kappa_{eg}$  and  $\kappa_{ef}$  dependent on  $\kappa_L$  but independent of  $\mathbf{x}$  and  $\Delta^q$  such that almost surely*

$$\|\nabla f^q(\mathbf{x}) - \nabla M^q(\mathbf{x})\| \leq \kappa_{eg} \Delta^q \text{ and } |f^q(\mathbf{x}) - M^q(\mathbf{x})| \leq \kappa_{ef} (\Delta^q)^2 \ \forall \mathbf{x} \in \mathcal{B}(\mathbf{x}; \Delta^q).$$

**Definition 3** (Cauchy reduction). *Given  $\mathbf{X}_k \in \mathbb{R}^d$ ,  $\Delta_k^q > 0$ ,  $q \in \{h, l\}$ , and a function  $M_k^q : \mathcal{B}(\mathbf{X}_k; \Delta_k^q) \rightarrow \mathbb{R}$  obtained following Definition 1,  $\mathbf{S}_k^c$  is called the Cauchy step if*

$$M^q(\mathbf{X}_k) - M^q(\mathbf{X}_k + \mathbf{S}_k^c) \geq \frac{1}{2} \|\nabla M^q(\mathbf{X}_k)\| \min \left\{ \frac{\|\nabla M^q(\mathbf{X}_k)\|}{\|\nabla^2 M^q(\mathbf{X}_k)\|}, \Delta_k^q \right\}.$$

When  $\|\nabla^2 M_k^q(\mathbf{X}_k)\| = 0$ , we assume  $\|\nabla M^q(\mathbf{X}_k)\|/\|\nabla^2 M^q(\mathbf{X}_k)\| = +\infty$ . The Cauchy step is derived by minimizing the model  $M_k^q(\cdot)$  along the steepest descent direction within  $\mathcal{B}(\mathbf{X}_k; \Delta_k^q)$ , making it easy and quick to compute.

**Definition 4** (filtration and stopping time). A filtration  $\{\mathcal{F}_k\}_{k \geq 1}$  on a probability space  $(\Omega, \mathbb{P}, \mathcal{F})$  is a sequence of  $\sigma$ -algebras, each contained within the next, such that for all  $k$ ,  $\mathcal{F}_k$  is a subset of  $\mathcal{F}_{k+1}$ , and all are subsets of  $\mathcal{F}$ . A function  $N : \Omega \rightarrow \{0, 1, 2, \dots, \infty\}$  is referred to as a stopping time with respect to the filtration  $\mathcal{F}$  if the set  $\{\omega \in \Omega : N(\omega) = n\}$  is an element of  $\mathcal{F}$  for every  $n < \infty$ .

### 2.3 Standing Assumptions

We now introduce the standing assumptions. Assumption 1 elucidates the characteristics of the functions  $f^h$  and  $f^l$ , enabling us to precisely pinpoint the problem we aim to address.

**Assumption 1** (function). The HF function  $f^h$  and the LF function  $f^l$  are twice continuously differentiable in an open domain  $\Omega$ ,  $\nabla f^h$  and  $\nabla f^l$  are Lipschitz continuous in  $\Omega$  with constant  $\kappa_{Lg} > 0$ , and  $\nabla^2 f^h$  and  $\nabla^2 f^l$  are Lipschitz continuous in  $\Omega$  with constant  $\kappa_L > 0$ .

We make the next assumption on the higher moments of the stochastic noise resembling the Bernstein condition. Random variables fulfilling Assumptions 2 exhibit a subexponential tail behavior.

**Assumption 2** (stochastic noise). The Monte Carlo oracles generate iid random variables  $F^q(\mathbf{X}_k^i, \xi_j) = f^q(\mathbf{X}_k^i) + E_{k,j}^{i,q}$  with  $E_{k,j}^{i,q} \in \mathcal{F}_{k,j}$  for  $i \in \{0, 1, 2, \dots, p, s\}$  and  $q \in \{h, l\}$ , where  $\mathbf{X}_k^s$  is the candidate iterate at iteration  $k$  and  $\mathcal{F}_k := \mathcal{F}_{k,0} \subset \mathcal{F}_{k,1} \subset \dots \subset \mathcal{F}_{k+1}$  for all  $k$ . Then the stochastic errors  $E_{k,j}^{i,q}$  are independent of  $\mathcal{F}_{k-1}$ ,  $\mathbb{E}[E_{k,j}^{i,q} | \mathcal{F}_{k,j-1}] = 0$ , and there exists  $(\sigma^q)^2 > 0$  and  $b^q > 0$  such that for a fixed  $n$ ,

$$\frac{1}{n} \sum_{j=1}^n \mathbb{E}[|E_{k,j}^{i,q}|^m | \mathcal{F}_{k,j-1}] \leq \frac{m!}{2} (b^q)^{m-2} (\sigma^q)^2, \quad \forall m = 2, 3, \dots, \forall k$$

### 2.4 Useful Results

In this section, we present useful results that will be invoked to prove the almost sure convergence of ASTRO-BFDF. The first result demonstrates that, under Assumption 2, the estimate of the stochastic errors is bounded by the square of the TR radius when a specific adaptive sampling rule is applied. Consequently, after a sufficiently large number of iterations, the true function  $f$  decreases whenever the candidate solution is accepted.

**Theorem 1** (Stochastic noise [15]). Let  $c_f > 0$  and  $\Delta_k^q > 0$  be given and  $E_{k,j}^{i,q}$  denotes the stochastic noise following Assumption 2 for  $q \in \{h, l\}$ . If the sample size  $N(\mathbf{X}_k^i)$  is determined by, for any  $\sigma_0 > 0$  and  $k \in \mathbb{N}$ ,

$$N(\mathbf{X}_k^i) = \min \left\{ n \in \mathbb{N} : \frac{\max\{\sigma_0, SV(\mathbf{X}_k^i, n)\}}{\sqrt{n}} \leq \frac{\kappa(\Delta_k^q)^2}{\sqrt{\lambda_k}} \right\}, \quad (7)$$

where  $\lambda_k = \mathcal{O}(\log k)$  and  $SV(\mathbf{X}_k^i, n)$  is a finite random variable that depends on sample size  $n$  and the design point  $\mathbf{X}_k^i$ , we obtain

$$\sum_{k=1}^{\infty} \mathbb{P} \left\{ \left| \frac{1}{N(\mathbf{X}_k^i)} \sum_{j=1}^{N(\mathbf{X}_k^i)} E_{k,j}^{i,q} \right| \geq c_f (\Delta_k^q)^2 \right\} < \infty.$$

Despite the fact that Theorem 1 has been proven with  $SV(\mathbf{X}_k^i, n) = \hat{\sigma}^h(\mathbf{X}_k^i, n)$  in Section 3.2 of [15], it can also be trivially established with a finite random variable  $SV(\mathbf{X}_k^i, n)$  by employing the same logical framework. The next result provides an upper bound for the gradient error norm at any design point within the TR when a stochastic linear or quadratic interpolation model is used. Combined with Theorem 1, it indicates that the gradient error norm will be bounded by the order of the TR radius after sufficiently many iterations.

**Lemma 1** (Stochastic Interpolation Model [11]). *If  $M_k^q(\mathbf{z})$  is a stochastic linear interpolation model or a stochastic quadratic interpolation model of  $f^q$  with the design set  $\mathcal{X}_k := \{\mathbf{X}_k^i\}_{i=0}^p \subset \mathcal{B}(\mathbf{X}_k; \Delta_k^q)$  and corresponding function estimates  $\bar{F}^q(\mathbf{X}_k^i, N(\mathbf{X}_k^i)) = f^q(\mathbf{X}_k^i) + \bar{E}_k^{i,q}(N_k^i)$  for  $q \in \{h, l\}$ , there exist positive constants  $\kappa_{eg1}$  and  $\kappa_{eg2}$  such that for any  $\mathbf{z} \in \mathcal{B}(\mathbf{X}_k; \Delta_k^q)$ ,*

$$\|\nabla M^q(\mathbf{z}) - \nabla f^q(\mathbf{z})\| \leq \kappa_{eg1} \Delta^q + \kappa_{eg2} \frac{\sqrt{\sum_{i=1}^p (\bar{E}_k^{i,q}(N_k^i) - \bar{E}_k^{0,q}(N_k^0))^2}}{\Delta^q}, \quad (8)$$

where  $\bar{E}_k^{i,q}(N_k^i) = N(\mathbf{X}_k^i)^{-1} \sum_{j=1}^{N(\mathbf{X}_k^i)} E_{k,j}^{i,q}$ .

Lastly, we present the variance of BFMC estimator. To make sure that the variance of BFMC is reduced, the second and third terms of the RHS of (9) should be less than zero for some  $n, v$ , and  $c$ . The another important thing we should notice is that  $\sigma^h(\mathbf{x}), \sigma^l(\mathbf{x})$ , and  $\sigma^{h,l}(\mathbf{x})$  are usually unknown in reality, forcing us to use the estimates such as  $\hat{\sigma}^h(\mathbf{x}, n), \hat{\sigma}^l(\mathbf{x}, \max\{n, v\})$ , and  $\hat{\sigma}^{h,l}(\mathbf{x}, \min\{n, v\})$ .

**Lemma 2** (Variance of BFMC [13]). *Let  $\mathbf{x} \in \mathbb{R}^d$ ,  $n, v \in \mathbb{N}$ , and  $c \in \mathbb{R}$ . Then the variance of the BFMC estimator  $\bar{F}^{\text{bf}}(\mathbf{x}, n, v, c)$  is*

$$\begin{aligned} \text{Var}(\bar{F}^{\text{bf}}(\mathbf{x}, n, v, c)) &= \frac{(\sigma^h(\mathbf{x}))^2}{n} + c^2 \left( \frac{1}{n} + \frac{1}{v} - 2 \frac{1}{\max\{n, v\}} \right) (\sigma^l(\mathbf{x}))^2 \\ &\quad + 2c \left( \frac{1}{\max\{n, v\}} - \frac{1}{n} \right) \sigma^{h,l}(\mathbf{x}), \end{aligned} \quad (9)$$

where  $\sigma^{h,l}(\mathbf{x})$  is a covariance between  $F^h(\mathbf{x}, \xi)$  and  $F^l(\mathbf{x}, \xi)$ .

**Remark 1.** *When  $v$  is less than or equal to  $n$ ,  $\text{Var}(\bar{F}^{\text{bf}}(\mathbf{x}, n, v, c))$  is bigger than or equal to  $\text{Var}(\bar{F}^h(\mathbf{x}, n))$ . Hence, a variance reduction is only available when  $v$  is bigger than  $n$ .*

### 3 Adaptive Sampling Bi-fidelity Trust Region Optimization

Similar to other stochastic TR algorithms, an adaptive sampling bi-fidelity TR algorithm (ASTRO-BFDF), stemming from ASTRO-DF [11], generates  $\{\mathbf{X}_k\}$  through the four steps outlined in Section 1.4. Notably, there exist two distinct components within ASTRO-BFDF, primarily attributable to the presence of a LF simulation oracle.

- (1) The sample sizes are intricately managed through adaptive sampling using BFMC or CMC. Within this approach, two critical decisions are made. Initially, as the samples stream in, the method discerns between employing CMC or BFMC. Secondly, it dynamically adjusts the sample sizes for both HF and LF simulation oracles, alongside determining the coefficient  $c$  in (3), all in real-time as the sample sizes increase.
- (2) At each iteration  $k$ , two local models can be constructed using HF and LF simulation oracles, respectively, each with its own TR:  $\Delta_k^l$  for the LF function and  $\Delta_k^h$  for the HF function. The local model utilizing the LF oracle serves two purposes: 1) identifying the candidate solution for the next iterate, and 2) updating the adaptive correlation constant determining the utilization of the local model for the LF function in Algorithm 3.

We first introduce the bi-fidelity adaptive sampling (BAS) strategy, which corresponds to the first feature.

---

**Algorithm 1**  $[N_k(\mathbf{x}), V_k(\mathbf{x}), C_k(\mathbf{x}), \tilde{F}_k(\mathbf{x})] = \text{BAS}(\mathbf{x}, \Delta_k, \lambda_k, \kappa, \mathcal{F}_k)$

---

**Input:**  $\mathbf{x} \in \mathbb{R}^d$ , TR radius  $\Delta_k$ , sample size lower bound sequence  $\{\lambda_k\}$ , batch size  $s^h$  and  $s^l$  for HF and LF simulation oracles, adaptive sampling constant  $\kappa > 0$ , and lower bound of an initial variance approximation  $\sigma_0 > 0$ .

- 1: Set  $n = (\sigma_0)^2 \lambda_k (\kappa^2 \Delta_k^4)^{-1}$  and  $v = n$ .
- 2: Estimate  $\hat{\sigma}^h(\mathbf{x}, n)$ ,  $\hat{\sigma}^{h,l}(\mathbf{x}, n)$ , and  $\hat{\sigma}^l(\mathbf{x}, v)$ .
- 3: Obtain the predicted sample sizes  $N^p$ , where

$$N^p(\mathbf{x}) = \min \left\{ n^p \in \mathbb{N} : \frac{\hat{\sigma}^h(\mathbf{x}, n)}{\sqrt{n^p}} \leq \frac{\kappa \Delta_k^2}{\sqrt{\lambda_k}} \right\} \quad (10)$$

- 4: **loop**
- 5:   Approximately compute  $C^*$ ,  $N^*$ , and  $V^*$  by solving the problem (11) and set  $c = C^*$ .
- 6:   **if**  $w^h N^* + w^l V^* \leq w^h N^p$  **then**
- 7:     Set  $v = \max\{n + 1, v\}$  and update  $\hat{\sigma}^{h,l}(\mathbf{x}, n)$  and  $\hat{\sigma}^l(\mathbf{x}, v)$  by calling the LF oracle.
- 8:     **if**  $\text{Var}(\bar{F}^{\text{bf}}(\mathbf{x}, n, v, c)) \leq \kappa^2 \Delta_k^4 \lambda_k^{-1}$  **then**
- 9:       **return**  $[n, v, c, \bar{F}^{\text{bf}}(\mathbf{x}, n, v, c)]$  (BFMC)
- 10:     **end if**
- 11:     **if**  $n \geq N^* - 1$  **then**
- 12:       Set  $v = v + s^l$  and get  $s^l$  additional replications of the LF oracle and update  $\tilde{\sigma}^l(\mathbf{x}, v)$ .
- 13:     **else**
- 14:       Set  $n = n + s^h$  and update  $\hat{\sigma}^h(\mathbf{x}, n)$  and  $\hat{\sigma}^{h,l}(\mathbf{x}, n)$  by calling the LF and HF oracles.
- 15:     **end if**
- 16:     **else**
- 17:       **if**  $n \geq N^p(\mathbf{x})$  **then**
- 18:         **return**  $[n, v, c, \bar{F}^h(\mathbf{x}, n)]$  (CMC)
- 19:       **end if**
- 20:       Set  $n = n + s^h$  and update  $\hat{\sigma}^h(\mathbf{x}, n)$  and  $N^p(\mathbf{x})$  by calling the HF oracle.
- 21:     **end if**
- 22: **end loop**

---

### 3.1 Adaptive Sampling for Bi-Fidelity Stochastic Optimization

While BFMC has the capability to reduce the variance of the function estimate, blindly employing BFMC may not always be advantageous. For example, when the expense of invoking the LF simulation oracle is comparable or marginally lower than that of the HF one, and the inherent variance of the LF simulation significantly exceeds that of the HF simulation, BFMC should be avoided. Therefore, it is essential to decide which Monte Carlo method to employ at a given design point based on the variance of the LF and HF simulation output and the covariance between them. However, a challenge is that the true variances of the LF and HF simulation output are unknown. Therefore, when adaptive sampling is utilized, the choice of the MC method needs to be dynamically determined based on variance and covariance estimates, which are sequentially updated using the simulation results. In summary, we should dynamically determine  $N$ ,  $V$ , and  $C$  while streaming the simulation replications, where  $N$  and  $V$  are the sample sizes for the HF and LF oracle and  $C$  represents the coefficient in the BFMC estimate, which is denoted as  $c$  in (3). To achieve this for any design point  $\mathbf{x}$  at iteration  $k$ , we suggest BAS, as listed in Algorithm 1.

Algorithm 1 starts by sampling  $n$  number of the HF oracle and the LF oracle to estimate the variance and covariance terms in (9). By leveraging the variance estimate  $\hat{\sigma}^h(\mathbf{x}, n)$ , we can derive a predicted minimum sample sizes  $N^p(\mathbf{x})$  for CMC, adhering to the adaptive sampling rule (7). Then the predicted computational cost of CMC at  $\mathbf{x}$  is represented as  $w^h N^p(\mathbf{x})$ , where  $w^h$  is the cost of calling HF oracle once. Our next step involves juxtaposing this against the projected computational costs of BFMC. To predict the lowest costs with corresponding sample sizes for BFMC, we solve (11) with variance estimates  $\hat{\sigma}^h(\mathbf{x}, n)$ ,  $\hat{\sigma}^l(\mathbf{x}, \max\{v, n\})$ , and  $\hat{\sigma}^{h,l}(\mathbf{x}, n)$  for  $\text{Var}(\bar{F}^{\text{bf}}(\mathbf{x}, \tilde{n}, \tilde{v}, \tilde{c}))$ .

$$\begin{aligned} [N^*, V^*, C^*] \in \operatorname{argmin}_{\tilde{n}, \tilde{v}, \tilde{c} \in \mathfrak{R}} \quad & w^h \tilde{n} + w^l \tilde{v} \\ \text{subject to} \quad & \text{Var}(\bar{F}^{\text{bf}}(\mathbf{x}, \tilde{n}, \tilde{v}, \tilde{c})) \leq \kappa^2 \Delta_k^4 \lambda_k^{-1} \\ & \tilde{n} - \tilde{v} \leq 0 \\ & n \leq \tilde{n} \leq \infty \\ & \max\{v, n\} \leq \tilde{v} < \infty, \end{aligned} \tag{11}$$

where  $w^l$  is the cost for calling LF oracle once. The first constraint is the adaptive sampling rule which originated from (7), ensuring that BFMC achieves the required accuracy. We are now poised to contrast the predicted computational costs between the crude MC and BFMC.

If  $w^h N^p \leq w^h N^* + w^l V^*$ , employing the CMC method would be more cost-effective in achieving the required accuracy of estimates at the current iteration, given the information available. Hence, if  $n \geq N^p$ , the accuracy of the function estimate is already sufficient to proceed the optimization and thus, the algorithm returns the function estimate with CMC ( $\bar{F}(\mathbf{x}, n)$ ). If not, we update  $\hat{\sigma}^h(\mathbf{x}, n = n + s^h)$  by calling  $s^h$  additional replications of the HF oracle. Then we proceed to Step 5 and continue with the algorithm using the newly updated  $n$  and variance estimates. It is worth to emphasize that the variance estimate for the LF function and the covariance estimate are not updated.

Following Step 5, if the cost of BFMC is lower than that of CMC, BFMC might offer greater cost-effectiveness, prompting the algorithm to proceed to Step 6. We first set  $v = \max\{v, n + 1\}$  with the updated  $n$  in Step 20 to ensure that  $v > n$  (See remark 1). Following this adjustment, additional replications of the LF oracle may become necessary due to the updated value of  $v$ . Consequently, it is imperative to update both  $\hat{\sigma}^l(\mathbf{x}, v)$  and  $\hat{\sigma}^{h,l}(\mathbf{x}, n)$  to reflect this change. Sub-

sequently, if the variance of the function estimate by BFMC is small enough compared to the optimality measure, i.e.,

$$\text{Var}(\bar{F}^{\text{bf}}(\mathbf{x}, n, v, c)) \leq \kappa^2 \Delta_k^4 \lambda_k^{-1}, \quad (12)$$

the algorithm returns  $\bar{F}^{\text{bf}}(\mathbf{x}, n, v, c)$ . If not, we need to decide whether to increase  $n$  or  $v$ . As evident from (9),  $n$  has a more pronounced impact on the left-hand side of (12) compared to  $v$ . Therefore, our initial assessment focuses on determining whether we need to increase  $n$  or not. If  $n < N^* - 1$ , we set  $n = n + s^h$  and update  $\hat{\sigma}^h(\mathbf{x}, n)$  and  $\hat{\sigma}^{h,l}(\mathbf{x}, n)$  by obtaining the necessary number of additional LF and HF simulation results. Subsequently, we move on to Step 5 and proceed with the algorithm utilizing the newly updated  $n$ . If  $n \geq N^* - 1$ , we acquire only  $s^l$  additional replications from the LF oracle and update  $\hat{\sigma}^l(\mathbf{x}, v)$ . Following this, we advance to Step 5 and continue the algorithm with the newly updated  $v$ .

Since  $n, v$ , and  $c$  are determined dynamically based on the realization of simulation results in Algorithm 1, three outputs are the stopping times determined by the filtration. Hence, we refer the output of Algorithm 1 as  $[N_k(\mathbf{x}), V_k(\mathbf{x}), C_k(\mathbf{x}), \tilde{F}_k(\mathbf{x})]$ .

**Remark 2.** *While employing CMC, the combined replications from the LF oracle can be reused for constructing the local model using the LF oracle, detailed in Section 3.2.*

### 3.2 Bi-fidelity Stochastic Trust Region Method

We now delve into the bi-fidelity stochastic TR method with the adaptive sampling method (ASTRO-BFDF). The fundamental concept of the suggested algorithm is to leverage the LF oracle until it no longer yields superior solutions for the HF function, exclusively relying on the LF oracle. Hence, unlike the stochastic TR methods discussed in Section 1.4, two different local models can be constructed utilizing two distinct TRs specifically tailored for HF and LF functions, referred to as  $\Delta_k^l$  for the LF one and  $\Delta_k^h$  for the HF one. It is noteworthy that  $\Delta_k^h$  is greater than  $\Delta_k^l$  for any iterations  $k \in \mathbb{N}$  to maintain large step sizes for the local model with the HF function and save computational budget in (12) and (10).

With two TRs, we should determine when and how to construct the local model for the LF function because the indiscriminate use of the LF oracle may lead to inefficiency. The challenge lies in our inability to pinpoint the specific region where the LF function proves beneficial in finding better solutions for the HF function without assessing both functions across the entire feasible domain. Some previous studies have attempted to address this by quantifying the correlation between the HF and LF functions through sampling various design points and their corresponding function estimates [16, 17]. However, as we will unveil in Section 5, it becomes evident that low correlation does not consistently signify the unhelpfulness of the LF function in optimization. Particularly, the TR method must ascertain the utility of the LF oracle within the TR, rather than across the entire feasible domain. Therefore, we propose the adoption of an adaptive correlation constant, represented as  $\alpha_k$ , to assess whether it is beneficial to construct  $M_k^l$  or not.

The adaptive correlation constant is dynamically updated, akin to the TR, leveraging results from previous iterations. This enables us to effectively quantify whether the LF function contributes to optimization within the current TR or not. In details, for each iteration  $k$ , we initially evaluate whether  $\alpha_k$  is larger than a user-defined threshold  $\alpha_{th} \in (0, 1)$  by invoking Algorithm 3 in Step 2 of Algorithm 2. If this condition is met, we construct  $M_k^l$  using solely a design set  $\mathcal{X}_k^l$  and corresponding LF function estimates. Next, we locate the candidate iterate by minimizing  $M_k^l$  within the TR  $\mathcal{B}(\mathbf{X}_k; \Delta_k^l)$ . If this candidate yields a sufficient decrease in the HF function and the gradient norm of the model is sufficiently large, it is accepted, the TR expands, and  $\alpha_k$

---

**Algorithm 2** ASTRO-BFDF

---

**Input:** Initial incumbent  $\mathbf{x}_0 \in \Re^d$ , initial and maximum TR radius  $\Delta_0^l, \Delta_0^h, \Delta_{\max} > 0$ , model fitness thresholds  $0 < \eta < 1$  and certification threshold  $\mu > 0$ , expansion and shrinkage constants  $\gamma_1 > 1$  and  $\gamma_2 \in (0, 1)$ , sample size lower bound sequence  $\{\lambda_k\} = \{\mathcal{O}(\log k)\}$ , adaptive sampling constant  $\kappa > 0$ , correlation constant  $\alpha_k > 0$ , and lower bound of an initial variance approximation  $\sigma_0^l > 0$ .

- 1: **for**  $k = 0, 1, 2, \dots$  **do**
- 2:   Obtain  $I_k^h, \mathbf{X}_k^s, \Delta_k^l$ , and  $\Delta_k^h$  by calling Algorithm 3.
- 3:   **if**  $I_k^h$  is True **then**
- 4:     Select  $\mathcal{X}_k = \{\mathbf{X}_k^i\}_{i=0}^{2d} \subset \mathcal{B}(\mathbf{X}_k; \Delta_k^h)$ .
- 5:     Estimate the HF function at  $\{\mathbf{X}_k^i\}_{i=0}^{2d}$  by calling Algorithm 1.
- 6:     Estimate the LF function  $\bar{F}^l(\mathbf{X}_k^i, T_k^i)$  at  $\{\mathbf{X}_k^i\}_{i=0}^{2d}$ , satisfying

$$T_k^i = \min \left\{ t \in \mathbb{N} : \frac{\max\{\sigma_0^l, \hat{\sigma}^l(\mathbf{X}_k^i, t)\}}{\sqrt{t}} \leq \frac{\kappa(\Delta_k^h)^2}{\sqrt{\lambda_k}} \right\}. \quad (13)$$

- 7:     Construct local models  $M_k^l(\mathbf{X})$  and  $M_k^h(\mathbf{X})$ .
- 8:     Approximately compute the local model minimizers

$$\mathbf{X}_k^{s,h} \in \operatorname{argmin}_{\|\mathbf{X} - \mathbf{X}_k\| \leq \Delta_k^h} M_k^h(\mathbf{X}) \text{ and } \mathbf{X}_k^{s,l} \in \operatorname{argmin}_{\|\mathbf{X} - \mathbf{X}_k\| \leq \Delta_k^h} M_k^l(\mathbf{X}).$$

- 9:     Estimate  $\tilde{F}(\mathbf{X}_k^{s,h})$  and  $\tilde{F}(\mathbf{X}_k^{s,l})$  by calling Algorithm 1 with  $\Delta_k = \Delta_k^h$ .
- 10:   Set the candidate point  $\mathbf{X}_k^s \in \operatorname{argmin}_{\mathbf{x} \in \{\mathbf{X}_k^{s,h}, \mathbf{X}_k^{s,l}\}} \tilde{F}(\mathbf{x})$ .
- 11:   Compute the success ratio  $\hat{\rho}_k$  and  $\hat{\rho}_k^l$  as

$$\hat{\rho}_k = \frac{\tilde{F}_k(\mathbf{X}_k^0) - \tilde{F}_k(\mathbf{X}_k^s)}{M_k^h(\mathbf{X}_k^0) - M_k^h(\mathbf{X}_k^s)} \text{ and } \hat{\rho}_k^l = \frac{\tilde{F}_k(\mathbf{X}_k^0) - \tilde{F}_k(\mathbf{X}_k^{s,l})}{M_k^l(\mathbf{X}_k^0) - M_k^l(\mathbf{X}_k^{s,l})}.$$

- 12:   If  $\hat{\rho}_k^l \geq \eta$ , set  $\alpha_k = \gamma_1 \alpha_k$ ; otherwise set  $\alpha_k = \gamma_2 \alpha_k$ .
- 13:   Set  $(\mathbf{X}_{k+1}, \Delta_{k+1}^h) =$

$$\begin{cases} (\mathbf{X}_k^s, \min\{\gamma_1 \Delta_k^h, \Delta_{\max}\}) & \text{if } \hat{\rho}_k \geq \eta \text{ and } \mu \|\nabla M_k^h(\mathbf{X}_k)\| \geq \Delta_k^h, \\ (\mathbf{X}_k, \gamma_2 \Delta_k^h) & \text{otherwise,} \end{cases}$$

- 14:   **else**
- 15:     Set  $(\mathbf{X}_{k+1}, \Delta_{k+1}^l) = (\mathbf{X}_k^s, \gamma_1 \Delta_k^l)$ ,  $\alpha_k = \min\{\gamma_1 \alpha_k, 1\}$  and  $k = k + 1$ .
- 16:   **end if**
- 17: **end for**

---

---

**Algorithm 3**  $[I_k^h, \mathbf{X}_k^s, \Delta_k^l, \Delta_k^h] = \text{ASTRO-LFDF}(\mathbf{X}_k)$ 


---

**Input:**  $\mathbf{X}_k, \Delta_k^l$ , model fitness thresholds  $0 < \eta < 1$  and certification threshold  $\mu > 0$ , sufficient reduction constant  $\theta > 0$ , expansion and shrinkage constants  $\gamma_1 > 1$  and  $\gamma_2 \in (0, 1)$ , sample size lower bound sequence  $\{\lambda_k\} = \{\mathcal{O}(\log k)\}$ , adaptive sampling constant  $\kappa > 0$ , correlation constant  $\alpha_k > 0$ , correlation threshold  $\alpha_{th} > 0$ , lower bound of an initial variance approximation  $\sigma_0^l > 0$ , sufficient reduction constant  $\zeta > 0$ , and gradient norm of the model lower bound  $\hat{\epsilon} > 0$ .

```

1: loop
2:   if  $\alpha_k < \alpha_{th}$  then
3:     Set  $I_k^h = \text{True}$  and  $\mathbf{X}_k^{s,l} = \mathbf{X}_k$ 
4:     break
5:   end if
6:   Select  $\mathcal{X}_k^l = \{\mathbf{X}_k^i\}_{i=0}^p \subset \mathcal{B}(\mathbf{X}_k; \Delta_k^l)$ .
7:   Estimate  $\bar{F}^l(\mathbf{X}_k^i, T_k^i)$  at  $\{\mathbf{X}_k^i\}_{i=0}^{2d}$ , satisfying (13) with  $\Delta_k^l$  instead  $\Delta_k^h$ .
8:   Construct local model  $M_k^l(\mathbf{X})$ .
9:   Approximately compute the local model minimizer

```

$$\mathbf{X}_k^{s,l} = \underset{\|\mathbf{X} - \mathbf{X}_k\| \leq \Delta_k^l}{\operatorname{argmin}} M_k^l(\mathbf{X}).$$

```

10:  Estimate  $\tilde{F}_k(\mathbf{X}_k^{s,l})$  and  $\tilde{F}_k(\mathbf{X}_k^0)$  by calling Algorithm 1 with  $\Delta_k = \Delta_k^l$ .
11:  Compute the success ratio  $\hat{\rho}_k$  as

```

$$\hat{\rho}_k = \frac{\tilde{F}_k(\mathbf{X}_k^0) - \tilde{F}_k(\mathbf{X}_k^{s,l})}{\max\{\zeta(\Delta_k^h)^2, M_k^l(\mathbf{X}_k^0) - M_k^l(\mathbf{X}_k^{s,l})\}}. \quad (14)$$

```

12:  if  $\hat{\rho}_k \geq \eta$  and  $\|\nabla M_k^l(\mathbf{X}_k^0)\| \geq \hat{\epsilon}$  then
13:    Set  $I_k^h = \text{False}$ 
14:    break
15:  end if
16:  Set  $\Delta_k^l = \gamma_2 \Delta_k^l$  and  $\alpha_k = \gamma_2 \alpha_k$ 
17: end loop
18: Set  $\Delta_k^h = \max\{\Delta_k^l, \Delta_k^h\}$ 
19: return  $[I_k^h, \mathbf{X}_k^s, \Delta_k^l, \Delta_k^h]$ 

```

---

increases. Additionally,  $\Delta_k^h$  is adjusted to be larger than  $\Delta_k^l$  at Step 18 in Algorithm 3, and we proceed to the next iteration  $k + 1$ . If not, the candidate is rejected, leading to the contraction of  $\Delta_k^l$ , a decrease in  $\alpha_k$ , and progression to Step 6 in Algorithm 3 to identify a superior candidate within the shrunken TR. This process continues until the algorithm concludes that the LF oracle cannot contribute to discovering a better solution, indicated by  $\alpha_k < \alpha_{th}$ .

**Remark 3.** In Algorithm 3, a sufficient reduction test (Step 11 and 12) is different with the one in Algorithm 2. Firstly, for a successful iteration, the reduction in function estimates must be larger than  $\zeta(\Delta_k^h)^2$  for some  $\zeta > 0$  (See Step 11). Secondly, the norm of the local model gradient should be bigger than  $\hat{\epsilon}$  (See Step 12). These conditions prevent us from accepting a candidate due to a very small reduction in the local model value in (14). Additionally, they ensure the almost

sure convergence of ASTRO-BFDF (See the proof of Theorem 2 in Section 4).

When Algorithm 3 fails to identify the next iterate, we construct the local model of the HF function ( $M_k^h$ ) in Algorithm 2. To select the design set  $\mathcal{X}_k$ , we aim to reuse as many previously visited design points from past iterations or those used while constructing  $M_k^l$  in the current iteration as possible. Subsequently, we estimate the value of the HF function by invoking Algorithm 1. This yields the HF function estimate  $\tilde{F}(\mathbf{X}_k^i)$  and the LF function estimate  $\bar{F}^l(\mathbf{X}_k^i, V_k^i)$  for any  $i \in \{0, 1, 2, \dots, |\mathcal{X}_k|\}$ . Then, we can additionally derive estimates for the LF function ( $\bar{F}^l(\mathbf{X}_k^i, T_k^i)$ ), aligning with the adaptive sampling rule (13). It is worth noting that when the estimates for the HF function are acquired through BFMC,  $V_k^i$  from Algorithm 1 inherently adhere to (13), i.e.,  $V_k^i \geq T_k^i$ , with a high probability. With  $\mathcal{X}_k$  and corresponding HF and LF function estimates, two distinct local models for the HF and LF functions are constructed, and two minimizers,  $\mathbf{X}_k^{s,l}$  and  $\mathbf{X}_k^{s,h}$ , are derived, with one stemming from  $M_k^l$  and the other from  $M_k^h$ . We evaluate the HF function values at two potential candidate points and designate the one with the lower objective value as the candidate point to go forward with. Leveraging this candidate, we update the next iterate and  $\Delta_k^h$ . Finally, the adaptive correlation constant is adjusted based on the results of the sufficient reduction test at  $\mathbf{X}_k^{s,l}$ .

In Algorithm 2, the creation of the local model for the LF function occurs at various points, each serving distinct purposes. Specifically, within Algorithm 3, which operates as the inner loop within Algorithm 2, we construct this model to seek an improved solution for the HF function. This decision stems from the belief that the LF function shares analogous gradient and curvature information, deduced from the insights gathered from previous iterations, denoted by  $\alpha_k > \alpha_{th}$ . Thus, the utilization of the HF oracle is minimized, being employed only for the sufficient reduction test. In the outer loop, the primary objective is to update the adaptive correlation constant, even in cases where the LF function has not proven beneficial in preceding iterations. In this case, our aim is to minimize reliance on the LF function, a goal achievable through the adoption of BFMC. When the HF function values are estimated at Step 5 in ASTRO-BFDF, an ample number of independent replications of the LF oracle are already obtained by BFMC. This enables the construction of  $M_k^l$  without incurring any additional computational burden. Unfortunately, in scenarios where the LF function fails to contribute meaningfully to the optimization process, Algorithm 2 may consume more resources compared to alternative solvers that exclusively utilize the HF function. However, discerning the utility of the LF function necessitates an additional computational budget, albeit the impact may be marginal in practice, as we will elaborate on in Section 5.

## 4 Convergence Analysis

In this section, we delve into demonstrating the convergence of ASTRO-BFDF. We first introduce two additional assumptions concerning the local model. Firstly, we stipulate that the minimizer of the local model must yield a certain degree of function reduction, known as the Cauchy reduction (See Definition 3). Secondly, the Hessian of the local model should be uniformly bounded. Both of these assumptions are essential to validate the quality of the candidate point for any given iteration  $k$ .

**Assumption 3** (Reduction in Subproblem). *For some  $\kappa_{fcd} \in (0, 1]$ ,  $q \in \{h, l\}$ , and all  $k$ ,  $M_k^q(\mathbf{X}_k^0) - M_k^q(\mathbf{X}_k^{s,q}) \geq \kappa_{fcd} (M_k^q(\mathbf{X}_k^0) - M_k^q(\mathbf{X}_k^0 + \mathbf{S}_k^c))$ , where  $\mathbf{S}_k^c$  is the Cauchy step.*

**Assumption 4** (Bounded Hessian in Norm). *In ASTRO-BFDF, the local model Hessians  $\mathbf{H}_k^q$  are bounded by  $\kappa_{\mathbf{H}}^q$  for all  $k$  and  $q \in \{h, l\}$  with  $\kappa_{\mathbf{H}}^q \in (0, \infty)$  almost surely.*

The convergence analysis of the adaptive sampling stochastic TR method for derivative-free optimization has received considerable attention in prior works such as [11, 15]. While our approach to proving the convergence shares similarities with those, there are two crucial considerations we must address.

- (a) (Stochastic noise) BFMC ought to yield results consistent with those of Theorem 1, indicating that the stochastic error in BFMC will indeed be less than  $\mathcal{O}((\Delta_k^q)^2)$  for  $q \in \{h, l\}$  after sufficiently large  $k$ . To achieve this, a crucial prerequisite (See Assumption 2) is ensuring that  $F^h(\mathbf{x}, \xi) - cF^l(\mathbf{x}, \xi)$  exhibits similar properties to  $F^h(\mathbf{x}, \xi)$  for any  $\xi \in \Xi$ ,  $c > 0$ , and  $\mathbf{x} \in \mathbb{R}^d$ .
- (b) (Trust-region) The TR sizes for both HF and LF functions need to converge to zero. In the context of convergence theory in the most stochastic TR methods [2, 4, 11], it becomes imperative to demonstrate that the TR radius converges to zero as  $k$  approaches  $+\infty$  in some probabilistic senses. This necessity arises because function estimate errors typically remain bounded by the order of the TR size, given specific sampling rules and assumptions. Consequently, the estimation errors will also converge to zero, ensuring the accuracy of the estimates. Therefore, within bi-fidelity stochastic optimization, we also need the same result for  $\Delta_k^h$ . Furthermore, since  $\Delta_k^h \geq \Delta_k^l$  for all  $k \in \mathbb{N}$ , the convergence of  $\Delta_k^h$  implies the convergence of  $\Delta_k^l$  as well.

Taking into account the aforementioned crucial considerations, we are now poised to present the convergence theory of ASTRO-BFDF.

**Theorem 2** (Almost Sure Convergence). *Let Assumptions 1-4 hold. Then,*

$$\lim_{k \rightarrow \infty} \|\nabla f^h(\mathbf{X}_k)\| \xrightarrow{w.p.1} 0. \quad (15)$$

Theorem 2 guarantees that a sequence  $\{\mathbf{X}_k(\omega)\}$  generated by Algorithm 2 converges to the first-order stationary point for any sample path  $\omega \in \Omega$ .

**Proof of Theorem 2** We start by demonstrating that the iid random variables  $E_{k,j}^{i,h} - cE_{k,j}^{i,l}$  also fulfill Assumption 2 for any  $k \in \mathbb{N}$ ,  $c \in \mathbb{R}$ , and  $i \in \{0, 1, 2, \dots, p, s\}$ , indicating their adherence to the sub-exponential distribution.

**Lemma 3.** *Let Assumption 2 holds. Then there exist  $\sigma^2 > 0$  and  $b > 0$  such that for a fixed  $n$  and  $c \in \mathbb{R}$ ,*

$$\frac{1}{n} \sum_{j=1}^n \mathbb{E}[|E_{k,j}^{i,h} - cE_{k,j}^{i,l}|^m \mid \mathcal{F}_{k,j-1}] \leq \frac{m!}{2} b^{m-2} \sigma^2, \quad \forall m = 2, 3, \dots, \forall k. \quad (16)$$

*Proof.* We obtain from the Minkowski inequality and Assumption 2 that for any  $k, j \in \mathbb{N}$ ,  $c \in \mathbb{R}$ , and any  $m \in \{2, 3, \dots\}$ , there exist  $b^h, b^l, (\sigma^h)^2, (\sigma^l)^2 > 0$  such that

$$\begin{aligned} \mathbb{E}[|E_{k,j}^{i,h} - cE_{k,j}^{i,l}|^m \mid \mathcal{F}_{k,j-1}] &\leq \left( \mathbb{E}[|E_{k,j}^{i,h}|^m \mid \mathcal{F}_{k,j-1}]^{\frac{1}{m}} + \mathbb{E}[|cE_{k,j}^{i,l}|^m \mid \mathcal{F}_{k,j-1}]^{\frac{1}{m}} \right)^m \\ &\leq \left( \left( \frac{m!}{2} (b^h)^{m-2} (\sigma^h)^2 \right)^{\frac{1}{m}} + \left( \frac{m!}{2} (b^l)^{m-2} (\sigma^l)^2 \right)^{\frac{1}{m}} \right)^m. \end{aligned} \quad (17)$$

Without loss of generality, let us assume that  $\sigma^h > \sigma^l > 0$  and  $b^h > b^l$ . Then there must exist some constant  $\alpha_\sigma, \alpha_b > 1$  such that  $\alpha_\sigma(\sigma^l)^2 = (\sigma^h)^2$  and  $\alpha_b b^l = b^h$ . Then the right-hand side of

(17) becomes  $((\alpha_\sigma^2 \alpha_b^{m-2})^{1/m} + 1)^m (2^{-1} m! (b^l)^{m-2} (\sigma^l)^2)$ . Since  $(\alpha_\sigma^2 \alpha_b^{m-2})^{1/m} + 1 \leq \alpha_\sigma \alpha_b + 1$  for all  $m \in \{2, 3, \dots\}$ , we obtain

$$\frac{1}{n} \sum_{j=1}^n \mathbb{E}[|E_{k,j}^{i,h} - cE_{k,j}^{i,l}|^m \mid \mathcal{F}_{k,j-1}] \leq \frac{m!}{2} ((\alpha_\sigma \alpha_b + 1) b^l)^{m-2} ((\alpha_\sigma \alpha_b + 1) \sigma^l)^2.$$

Hence, the statement of the theorem holds with  $\sigma = \sigma^l (\alpha_\sigma \alpha_b + 1)$  and  $b = (\alpha_\sigma \alpha_b + 1) b^l$ .  $\square$

Now let us prove that the function estimate error from BAS is bounded by  $\mathcal{O}((\Delta_k^h)^2)$ , aligning with the outcome stated in Theorem 1. This finding not only enables us to attain the stochastic fully linear model (See Definition 2) but also leads to the crucial observation that  $\Delta_k^h$  converges to 0 almost surely as  $k$  tends to infinity.

**Lemma 4.** *Let Assumption 2 holds and  $\mathbf{X}_k^i$  for  $i \in \{0, 1, 2, \dots, p, s\}$  be the design points generated by Algorithm 2 at iteration  $k$ . Let  $\tilde{F}(\mathbf{X}_k^i) = f(\mathbf{X}_k^i) + \bar{E}_k^i$  be the HF function estimate obtained from Algorithm 1 with  $\Delta_k = \Delta_k^q$  for  $q \in \{h, l\}$ . Then, given  $c_f > 0$ ,*

$$\mathbb{P}\{|\tilde{E}_k^i| \geq c_f (\Delta_k^q)^2 \text{ i.o.}\} = 0. \quad (18)$$

*Proof.* Let  $\omega \in \Omega$ . Firstly, if the function estimate from BAS was obtained by CMC, we know from Theorem 1 that the statement of the lemma is satisfied. Now, we assume that the function estimate  $\tilde{F}(\mathbf{X}_k^i)$  is obtained using BFMC, implying that

$$|\tilde{E}_k^i(\omega)| = |\bar{E}_k^{i,h}(N_k^i(\omega)) - C_k(\omega) \bar{E}_k^{i,l}(N_k^i(\omega)) + C_k(\omega) \bar{E}_k^{i,l}(V_k^i(\omega))|,$$

where  $N_k^i = N_k(\mathbf{X}_k^i)$ ,  $V_k^i = V_k(\mathbf{X}_k^i)$ , and  $\bar{E}_k^{i,q}(N_k^i) = N(\mathbf{X}_k^i)^{-1} \sum_{j=1}^{N(\mathbf{X}_k^i)} E_{k,j}^{i,q}$  for  $q \in \{h, l\}$ . To simplify notation, we will omit  $\omega$  from this point forward. Then we have

$$\mathbb{P}\{|\tilde{E}_k^i| \geq c_f (\Delta_k^q)^2 \mid C_k = c\} \leq \mathbb{P}\{|\bar{E}_k^{i,h}(N_k^i) - c \bar{E}_k^{i,l}(N_k^i)| \geq \frac{c_f}{2} (\Delta_k^q)^2\} + \mathbb{P}\{|c \bar{E}_k^{i,l}(V_k^i)| \geq \frac{c_f}{2} (\Delta_k^q)^2\}. \quad (19)$$

We know from Step 1 and 8 in Algorithm 1, Lemma 2, and  $N_k^i < V_k^i$  that we obtain  $N_k^i, V_k^i$ , and  $c$  such that

$$\frac{\max\{\sigma_0, \sqrt{(\hat{\sigma}^h(\mathbf{X}_k^i, N_k^i))^2 + c^2(\hat{\sigma}^l(\mathbf{X}_k^i, V_k^i))^2 - 2c\hat{\sigma}^{h,l}(\mathbf{X}_k^i, N_k^i)}\}}{\sqrt{N_k^i}} \leq \frac{\kappa(\Delta_k^q)^2}{\sqrt{\lambda_k}},$$

and

$$\frac{\max\{\sigma_0, \sqrt{2c\hat{\sigma}^{h,l}(\mathbf{X}_k^i, N_k^i) - c^2(\hat{\sigma}^l(\mathbf{X}_k^i, V_k^i))^2}\}}{\sqrt{V_k^i}} \leq \frac{\kappa(\Delta_k^q)^2}{\sqrt{\lambda_k}},$$

for some  $\sigma_0 > 0$ . We also know from Lemma 3 that Assumption 2 holds for  $E_{k,0}^{i,h} - cE_{k,0}^{i,l}$ , implying that Theorem 1 holds for  $E_{k,0}^{i,h} - cE_{k,0}^{i,l}$ . Hence, the right-hand side of (19) is summable, from which we obtain  $\mathbb{P}\{|\tilde{E}_k^i| \geq c_f (\Delta_k^q)^2\}$  is also summable based on  $\mathbb{P}\{|\tilde{E}_k^i| \geq c_f (\Delta_k^q)^2\} = \mathbb{E}[\mathbb{P}\{|\tilde{E}_k^i| \geq c_f (\Delta_k^q)^2 \mid C_k = c\}]$ . As a result, the statement of the theorem holds.  $\square$

Next, we demonstrate that as  $k$  goes to infinity, both TR radii inevitably converge to zero almost surely. Despite the main framework of our proof differing trivially from the one presented in [4], we opt to provide a comprehensive proof to facilitate understanding in Appendix A.

**Lemma 5.** *Let Assumptions 1-4 hold. Then,*

$$\Delta_k^h \xrightarrow{w.p.1} 0 \text{ and } \Delta_k^l \xrightarrow{w.p.1} 0 \text{ as } k \rightarrow \infty.$$

*Proof.* See Appendix A. □

Relying on Lemma 5, we show through Lemma 6 that the gradient of the model for the HF function converges to a true gradient almost surely. It is worth highlighting that the local model for the HF function is not constructed at every iteration, as sometimes the local model for the LF function can discover a better solution.

**Lemma 6.** *Let Assumptions 1-4 hold. Let  $\{k_j\}$  be the subsequence such that  $I_{k_j}^h = \text{True}$ . Then,*

$$\|\nabla M_{k_j}^h(\mathbf{X}_{k_j}^0) - \nabla f(\mathbf{X}_{k_j}^0)\| \xrightarrow{w.p.1} 0 \text{ as } j \rightarrow \infty.$$

*Proof.* We know from Lemma 4 that given  $c_f > 0$ , there exists sufficiently large  $J$  such that  $|\tilde{E}_{k_j}^i| < c_f(\Delta_{k_j}^h)^2$  for any  $i \in \{0, 1, \dots, p, s\}$  and  $j > J$ . Then from Lemma 1, we have,

$$\begin{aligned} \|\nabla M_{k_j}^h(\mathbf{X}_{k_j}^0) - \nabla f(\mathbf{X}_{k_j}^0)\| &\leq \kappa_{eg1}\Delta_{k_j}^h + \kappa_{eg2} \frac{\sqrt{\sum_{i=1}^p (\tilde{E}_{k_j}^i - \tilde{E}_{k_j}^0)^2}}{\Delta_{k_j}^h} \\ &\leq \kappa_{eg1}\Delta_{k_j}^h + \kappa_{eg2} \frac{|\tilde{E}_{k_j}^i - \tilde{E}_{k_j}^0|}{\Delta_{k_j}^h} \\ &\leq (\kappa_{eg1} + 2\kappa_{eg2}c_f)\Delta_{k_j}^h. \end{aligned}$$

Given that Lemma 5 ensures  $\Delta_{k_j}^h$  converges to 0 w.p.1, the statement of the theorem holds. □

In the following lemma, we demonstrate that after a sufficient number of iterations, if the TR for the HF function is relatively smaller than the model gradient, the iteration is successful with probability one. Given Lemma 6, Lemma 7 suggests that in cases where the true gradient is greater than zero, if the TR radius for the HF function is comparatively smaller than the true gradient, the candidate solution is accepted and the TR is expanded. This ensures that the TR for the HF function will not converge to zero before the true gradient does.

**Lemma 7.** *Let Assumptions 1-4 hold. Then there exists  $c_d > 0$  such that*

$$\mathbb{P} \left\{ \left( \Delta_k^h \leq c_d \|\nabla M_k^h(\mathbf{X}_k^0)\| \right) \cap (\hat{\rho}_k < \eta) \text{ i.o.} \right\} = 0.$$

*Proof.* We first note that for any  $k \in \mathbb{N}$ , when the minimizer of the low fidelity local model in Algorithm 3 is accepted as a next iterate, i.e.,  $I_k^h$  is False, we already have  $\hat{\rho}_k \geq \eta$ . Otherwise, the HF local model is constructed in Algorithm 2. Then the rest of the proof trivially follows from Lemma 4.4 with the adaptive sampling rule (A-0) in [15].

□

**Lemma 8.** *Let Assumptions 1-4 hold. Then*

$$\liminf \|\nabla f^h(\mathbf{X}_k)\| \xrightarrow{w.p.1} 0 \text{ as } k \rightarrow \infty. \quad (20)$$

*Proof.* Using Lemma 6 and 7, the proof can be completed by straightforwardly following the steps outlined in Theorem 4.6 of [4].  $\square$

We have now reached a point where we can confidently establish the almost sure convergence of ASTRO-BFDF. The following proof solidifies our claim.

*Proof of Theorem 2.* We first need to assume that there is a subsequence that has gradients bounded away from zero for contradiction. Particularly, suppose that there exists a set,  $\hat{\mathcal{D}}$ , of positive measure,  $\omega_1 \in \hat{\mathcal{D}}$ ,  $\epsilon_0 > 0$ , and a subsequence of successful iterates,  $\{t_j(\omega_1)\}$ , such that  $\|\nabla f^h(\mathbf{X}_{t_j(\omega_1)}(\omega_1))\| > 2\epsilon_0$ , for all  $j \in \mathbb{N}$ . We denote  $t_j = t_j(\omega_1)$  and suppress  $\omega_1$  in the following statements for ease of notation. Due to the lim-inf type of convergence just proved in (20), for each  $t_j$ , there exists a first successful iteration,  $\ell_j := \ell(t_j) > t_j$ , such that, for large enough  $k$ ,

$$\|\nabla f^h(\mathbf{X}_k)\| > 2\epsilon_0, \quad t_j \leq k < \ell_j, \quad (21)$$

and

$$\|\nabla f^h(\mathbf{X}_{\ell_j})\| < 1.5\epsilon_0. \quad (22)$$

Define  $\mathcal{A}_j^h := \{k \in \mathcal{H} : t_j \leq k < \ell_j\}$  and  $\mathcal{A}_j^l := \{k \in \mathcal{L} : t_j \leq k < \ell_j\}$ . Let  $j$  be sufficiently large and let  $k \in \mathcal{A}_j^h$ . We then obtain from Lemma 6

$$\|\nabla M_k^h(\mathbf{X}_k)\| > \epsilon_0. \quad (23)$$

Since  $k$  is a successful iteration,  $\hat{\rho}_k \geq \eta$ . Furthermore, Assumption 3 and (23) then imply that

$$\begin{aligned} f^h(\mathbf{X}_k) - f^h(\mathbf{X}_{k+1}) + \tilde{E}_k^0 - \tilde{E}_k^s &\geq \eta[M_k^h(\mathbf{X}_k) - M_k^h(\mathbf{X}_{k+1})] \\ &\geq \frac{1}{2}\eta\kappa_{fcd}\|\nabla M_k^h(\mathbf{X}_k)\| \min \left\{ \frac{\|\nabla M_k^h(\mathbf{X}_k)\|}{\|\mathbf{H}_k\|}, \Delta_k^h \right\} \\ &> c_{fd}\Delta_k^h, \end{aligned} \quad (24)$$

where  $c_{fd} = \frac{1}{2}\eta\kappa_{fcd}\min\{\epsilon_0, \hat{\epsilon}\}$ . When  $k \in \mathcal{A}_j^l$ , we also obtain the similar result with (24) using  $\|\nabla M_k^l(\mathbf{X}_k)\| > \hat{\epsilon}$ :

$$f^h(\mathbf{X}_k) - f^h(\mathbf{X}_{k+1}) + \tilde{E}_k^0 - \tilde{E}_k^s > c_{fd}\Delta_k^l. \quad (25)$$

Since we know from Lemma 4 that

$$|\tilde{E}_k^0 - \tilde{E}_k^s| < 0.5c_{fd}\Delta_k^h \text{ for } k \in \mathcal{A}_j^h \text{ and } |\tilde{E}_k^0 - \tilde{E}_k^s| < 0.5c_{fd}\Delta_k^l \text{ for } k \in \mathcal{A}_j^l, \quad (26)$$

the sequence  $\{f^h(\mathbf{X}_k)\}_{k \in \mathcal{A}_j}$  is monotone decreasing for sufficiently large  $j$ . From (25), (26), and the fact that  $\|\mathbf{X}_k - \mathbf{X}_{k+1}\| \leq \Delta_k$  for all  $k$ , we deduce that

$$\begin{aligned} \|\mathbf{X}_{t_j} - \mathbf{X}_{\ell_j}\| &\leq \sum_{i \in \mathcal{A}_j} \|\mathbf{X}_i - \mathbf{X}_{i+1}\| \leq \sum_{i \in \mathcal{A}_j^h} \Delta_i^h + \sum_{i \in \mathcal{A}_j^l} \Delta_i^l \\ &\leq \frac{2(f^h(\mathbf{X}_{t_j}) - f^h(\mathbf{X}_{\ell_j}))}{c_{fd}}. \end{aligned} \quad (27)$$

Now define  $\mathcal{C}_j := \{k \in \mathcal{K} : \ell_j \leq k < t_{j+1}\}$ . Let  $k \in \mathcal{C}_j$  for sufficiently large  $j$ . From (24)-(26), we then obtain

$$f^h(\mathbf{X}_k) - f^h(\mathbf{X}_{k+1}) \geq 0.5c_{fd}(\Delta_k^l)^2,$$

implying that the sequence  $\{f^h(\mathbf{X}_k)\}_{k \in \mathcal{A}_j \cup \mathcal{B}_j}$  is monotone decreasing for sufficiently large  $j$ . The boundedness of  $f^h$  from below then implies that the right-hand side of (27) converges to 0 as  $j$  goes to infinity, concluding that  $\lim_{j \rightarrow \infty} \|\mathbf{X}_{t_j} - \mathbf{X}_{\ell_j}\| = 0$ . Consequently, by continuity of the gradient, we obtain that  $\lim_{j \rightarrow \infty} \|\nabla f^h(\mathbf{X}_{t_j}) - \nabla f^h(\mathbf{X}_{\ell_j})\| = 0$ . However, this contradicts  $\|\nabla f^h(\mathbf{X}_{t_j}) - \nabla f^h(\mathbf{X}_{\ell_j})\| > 0.5\epsilon_0$ , obtained from (21) and (22). Thus, (15) must hold.  $\square$

## 5 Numerical Experiments

We will now assess and compare ASTRO-BFDF with other simulation optimization solvers. Our focus lies on testing across two distinct problem categories: synthetic problems and toy problems with Discrete Event Simulation (DES).

Synthetic problems constitute deterministic problems embellished with artificial stochastic Gaussian noise. Given our knowledge of the closed equation of  $f^h$ , generating numerous problems that adhere to predetermined assumptions becomes relatively straightforward. However, since both the function  $f^h$  and the stochastic noises are artificially generated, the performance of the solvers on these problems might not be indicative of its efficacy in handling real-world problems. In particular, when the same random number stream is used, the stochastic noises at different design points will be identical, implying that  $F^h(\cdot, \xi) - f^h(\cdot)$  is a constant function given fixed  $\xi \in \Xi$ . This setting satisfies a stricter assumption than the one posed in this paper. Hence, we also evaluated the solvers on toy problems utilizing DES to ensure testing with more realistic scenarios. DES simulates real-world conditions, generating multiple outputs utilized within the objective function  $f$ . All experiments have been implemented using SimOpt [18].

We compare ASTRO-BFDF, ASTRO-DF, ADAM [19], and Nelder-Mead [20]. In implementing the solvers, including ASTRO-BFDF, we applied Common Random Numbers (CRN), which involves using the same random number stream to reduce variance when comparing function estimates at different design points. To integrate CRN into ASTRO-BFDF, each time a local model is constructed, the sample sizes and the coefficient at the center point, obtained through BAS, are preserved and subsequently utilized for estimating the function values at other design points.

### 5.1 Synthetic Problems

We have evaluated four distinct deterministic equations for  $f^h$ , creating a total of 108 test problems by altering the LF function and incorporating different stochastic noises. Specifically, each problem utilizes a HF function defined as  $F^h(\cdot, \xi) = f^h(\cdot) + E^h(\cdot, \xi)$ , and a LF function represented as  $F^l(\cdot, \xi) = g_1(\kappa_{cor})g_2(f^h(\cdot)) + (E^h(\cdot, \xi) + E^l(\cdot, \xi))/2$ , where  $g_1$  and  $g_2$  are smooth functions.  $E^h(\cdot, \xi)$  and  $E^l(\cdot, \xi)$  represent stochastic noises, and  $\kappa_{cor}$  is a constant that adjusts the correlation between the HF and LF functions, which ranges from 0 to 1. Details about three deterministic problems (BRANIN, COLVILLE, FORRETTAL) can be found in [17], while the last problem, the Rosenbrock function (ROSEN) for bi-fidelity optimization, is introduced in [21]. We have tested the problems with three different values of  $\kappa_{cor}$ : 0.1, 0.5, and 0.9. Regarding the stochastic noises, a more complex setup is required to determine whether BAS can enhance computational efficiency. For instance, test problems should include an instance with a high variance of the LF oracle, which can make BFMC undesirable during the optimization. Thus, we examined the configuration in

which the stochastic noises for the HF and LF oracles adhere to the standard Gaussian distribution  $\mathcal{N}(0, c_{sd}^h)$  for  $c_{sd}^h \in \{20, 30, 40\}$  and Gaussian distribution  $\mathcal{N}(0, c_{sd}^l)$  for  $c_{sd}^l \in \{20, 30, 40\}$  respectively.

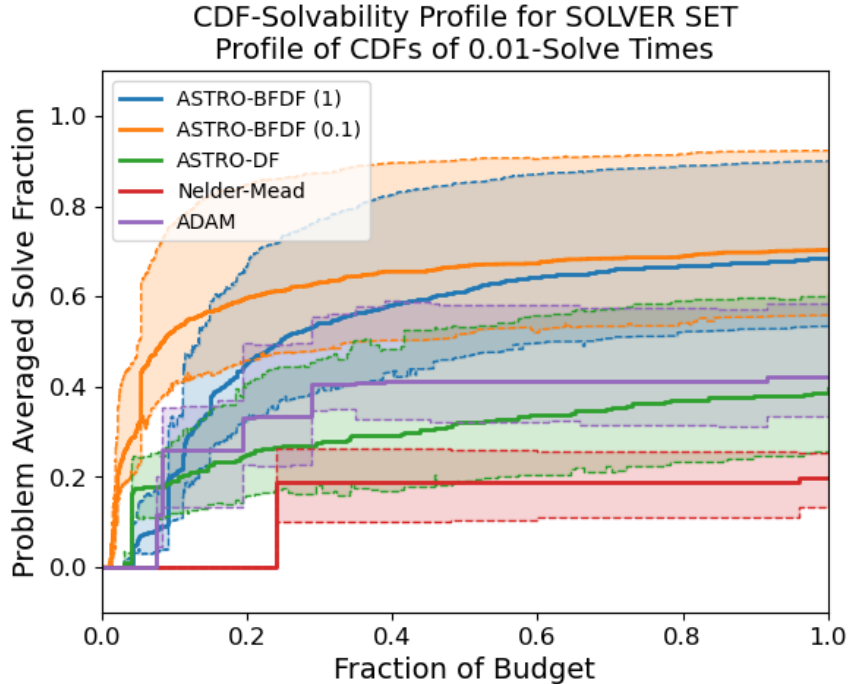


FIGURE 2: Fraction of 108 synthetic problems solved to 0.01-optimality with 95% confidence intervals from 20 runs of each algorithm shows a clear advantage in finite-time performance of ASTRO-BFDF.

Solvability profiles are used to compare the solvers, as illustrated in Figure 2. These profiles provide insights into how well a solver performs by showing the proportion of tested problems it solves within a certain relative optimality gap. Calculating this gap requires the optimal solution, which is determined as the best solution among all solvers for a given problem in practice. When the cost ratio of calling HF and LF oracles stands at 1:0.1, ASTRO-BFDF emerges as a standout performer, solving over 50% of the problems within a mere 15% of the budget. What is particularly noteworthy is that even when the costs for the LF function match those for the HF function (cost ratio 1:1), ASTRO-BFDF demonstrates faster convergence than ASTRO-DF. This suggests that utilizing the LF function could be beneficial for optimization, even if optimizing it requires a larger computational budget compared to optimizing the HF function. Hence, we will next delve deeper into the specific scenarios where leveraging the LF function proves advantageous for optimization.

**Usefulness of the LF function** Most papers [16, 17] employ the correlation between the LF and HF functions or the LF and the surrogate model to determine whether employing the LF oracle can be helpful for the optimization or not. However, the correlation can be varied based on the region we try to quantify. For instance, even though the LF function may exhibit a high correlation with the HF function in specific feasible regions, its usefulness can vary based on the optimization progress and setup, such as the initial design point. Hence, the correlation might not be suitable metric to determine whether the LF function is helpful for the optimization. Indeed, instead of requiring high correlation within the entire feasible region, having an accurate gradient

at the current iterate is sufficient to find a better solution, utilizing any available information source. This rationale underpins the use of an adaptive correlation constant in ASTRO-BFDF, which is updated based on whether the previous gradient estimates from the LF oracle have improved the solution.

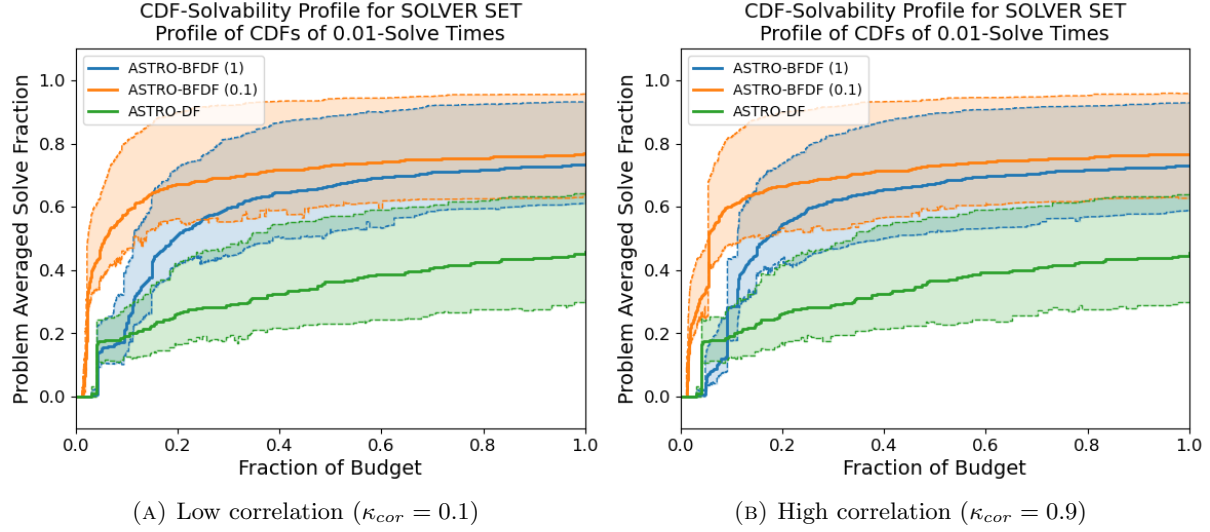


FIGURE 3: Solvability profiles of 36 problems with 95% confidence intervals from 20 runs of each algorithm with two different correlation setting between the LF and HF functions.

In Figure 3, ASTRO-BFDF consistently demonstrates superiority regardless of the correlation between the HF and LF functions. Particularly, when the correlation is relatively low, although the confidence interval of the fraction becomes large until 20% of the budget compared to the case with the high correlation, ASTRO-BFDF still shows faster convergence and maintains robust performance compared to ASTRO-DF.

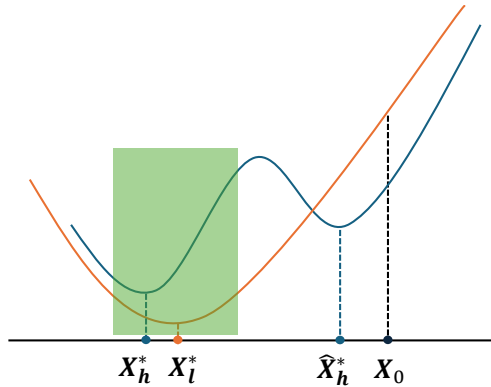


FIGURE 4: The illustration depicts the scenario where the LF function is convex.  $\mathbf{X}_h^*$  and  $\mathbf{X}_l^*$  represent the global optima of the HF and LF functions, respectively, while  $\mathbf{X}_0$  marks the initial iterate. Depending on the step size, using only the HF function may lead  $\mathbf{X}_k$  to converge to a local optimum ( $\hat{\mathbf{X}}_h^*$ ). However, if the LF function is used until the iterate reaches the green area, achieving the global optimum becomes possible.

The usefulness of the LF function in providing accurate gradient estimates can be maximized when it possesses unique structural properties, such as convexity, which could aid in locating the global optimum of the non-convex HF function (See Figure 4). In this case, the bi-fidelity optimization still remains advantageous despite high variance and costs of the LF oracle. However, it is important to note that the opposite scenario is also possible, where the optimum of the LF function is located near the local optimum of the HF function, which is undesirable (See Figure 1).

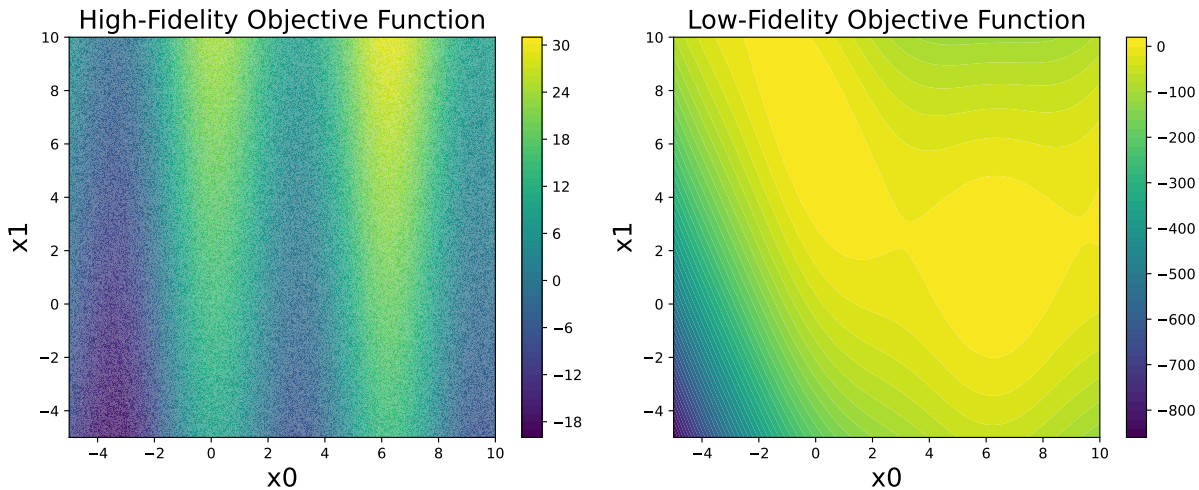


FIGURE 5: The contour maps of the HF and LF function without stochastic noises of the BRANIN problem with  $\kappa_{cor} = 1$ .

The Branin function is an example for which the bi-fidelity optimization is helpful due to the structure of the LF function. In Figure 5, even though the LF function is non-convex, it possesses a favorable structure that allows gradient-based methods to find the global optimum more easily compared to the HF function. Hence, during the optimization, the solver can find the solution near the global optimum of the HF function by leveraging only the LF function.

**Remark 4.** *The trajectory of ASTRO-BFDF toward a local optimum closely hinges on two critical factors: the initial design point and the parameter  $\alpha_0$ . Take, for instance, the scenario where the LF function typically pinpoints near the global optimum in the HF function like the BRANIN problem. Yet, if we kick off ASTRO-BFDF with an initial solution like (7,8), it is quite likely that ASTRO-BFDF converges towards points nearby, perhaps around (4,10) or (9,10). Moreover, when  $\alpha_0 < \alpha_{th}$ , the optimization at iteration 0 leans on the HF function, potentially leading the iterates to converge to a distinct local optimum compared to the path followed when  $\alpha_0 > \alpha_{th}$ . In our numerical experiments, we deliberately set  $\alpha_0 > \alpha_{th}$  to maximize the computational efficiency.*

## 5.2 Toy Problems with DES

In this section, we tested more realistic problems using DES for the HF and LF simulation oracles. We have tested two problems: a M/M/1 queue problem (M/M/1) and an inventory problem (SSCONT). In both cases, the DES model operates until a defined end time, denoted as  $T$ , thereby enabling the acquisition of multi-fidelity results through variations in  $T$ . Take, for instance, the scenario where the goal is to minimize inventory costs over 365 days. While the HF model simulates the entire 365-day inventory system, the LF simulation model can effectively mimic the

HF model's behavior over a shorter duration, say 110 days. In this specific instance, the cost ratio between the HF and LF models stands at 1 : 0.3. A notable aspect of this problem is that running one replication of the HF model inherently produces one replication of the LF model without incurring any additional computational expenses.

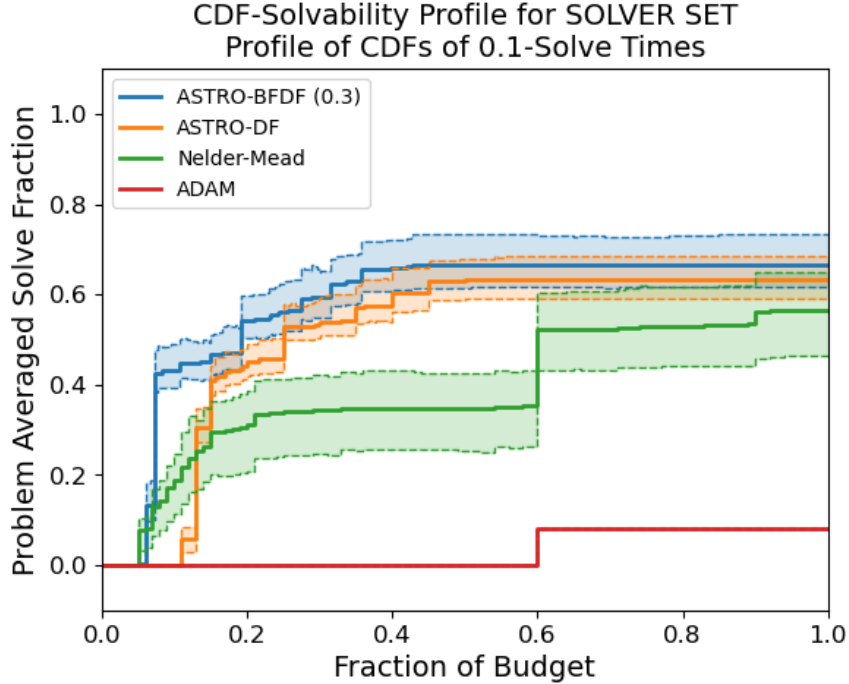


FIGURE 6: Fraction of 25 toy problems with DES solved to 0.1-optimality with 95% confidence intervals from 20 runs of each algorithm. ASTRO-BFDF demonstrates not only a faster convergence but also an enhanced ability to identify superior solutions by the end of the allocated computational budget.

Before delving into the details of each problem, we provide the solvability profile with 25 instances (See Figure 6), specifically including 5 instances from MM1 and 20 instances from SSSCONT. The cost ratio between the HF and LF models for both problems is 1 : 0.3, indicating that the LF oracle simulates the system for  $0.3T$  days.

### 5.2.1 M/M/1 Queue Problem

We employ a model that simulates a M/M/1 queue, characterized by an exponential distribution for both interarrival and service times. Let us denote the rate parameters of these as  $\mu$  for interarrival and  $\lambda$  for service time. The objective here is to minimize both the expected average sojourn time and a penalty, represented by  $0.1\mu^2$ , where  $\mu$  acts as the decision variable. One of the important characteristic of the problem is that  $F^h(\cdot, \xi)$  and  $F^l(\cdot, \xi)$  are smooth functions for any  $\xi \in \Xi$ , which can be verified by Figure 7. The difficulty in addressing this problem with the LF function lies in the fact that its gradient is relatively smaller compared to that of the HF function, which becomes clearer when we have larger  $\lambda$  (See Figure 7c and 7d). In Algorithm 3, the criterion for successful iterations hinges on comparing the reduction in model and function estimates. Therefore, when the gradient of the LF function is small, a candidate point can be accepted, albeit leading away from the optimal solution (Refer Remark 3).

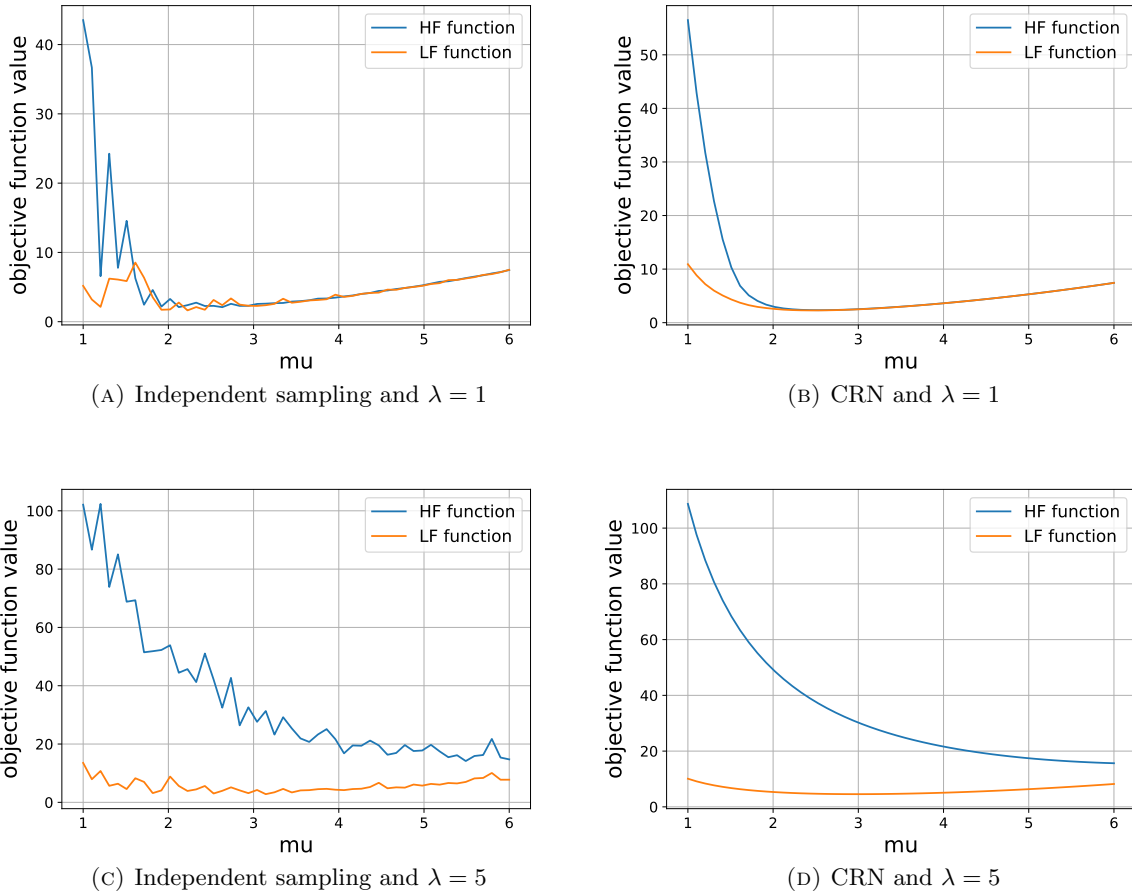


FIGURE 7: The trajectory of the objective function of the M/M/1 problem with and without CRN. When employing CRN, the objective function exhibits smoothness, indicating that both  $E^h(\cdot, \xi)$  and  $E^l(\cdot, \xi)$  are smooth functions for any  $\xi \in \Xi$ .

We have conducted testing on 5 instances of the M/M/1 problem, varying  $\lambda$  across the range  $\{1, 2, \dots, 5\}$  in Figure 6. Figure 8 illustrates the optimization progress for two scenarios: one where  $\lambda = 1$  and another where  $\lambda = 5$ . In the scenario where  $\lambda = 1$ , as the incumbents approach the optimal solution, it becomes essential for the TR to contract appropriately in order to achieve an accurate gradient approximation. While contracting the TR, ASTRO-DF exhausts its budget entirely, which explains its slower convergence in Figure 8a. In contrast, ASTRO-BFDF is capable of rapidly identifying a near-optimal solution. The primary reason is that the gradient of the local model for the LF function is inherently small, enabling us to sustain successful iterations before the TR initiates sequential contraction. Conversely, when  $\lambda = 5$ , the gradient of the local model for the LF function becomes exceedingly minuscule, prompting a cessation of LF function utilization after just a few iterations. Hence, in Figure 8b, the optimization trajectory of ASTRO-BFDF appears similar to that of ASTRO-DF, but ASTRO-BFDF demonstrates slightly faster convergence due to the variance-reduced function estimates provided by BAS.

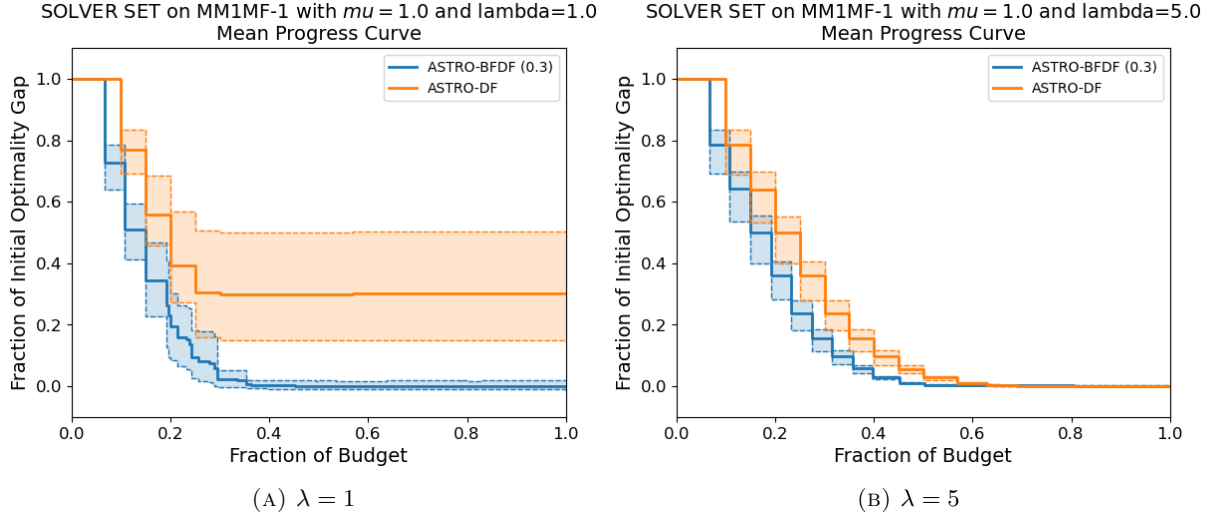


FIGURE 8: Fraction of the optimality gap with 95% confidence intervals from 20 runs of each algorithm.

### 5.2.2 $(s, S)$ Inventory Problem

In the inventory problem, we consider  $(s, S)$  inventory model with full backlogging. At each time step  $t$ , the demand  $D_t$ , which follows the exponential distribution with  $\mu_D$ , is generated. At the end of each time step, the inventory level is calculated and if it is below  $s$ , an order to get back up to  $S$  is placed. Lead times follow the Poisson distribution with mean  $\mu_L$  time steps. The optimization is to find the best  $s$  and  $S$  for minimizing the average costs, which is composed of backorder costs, order costs, and holding costs. This problem is significantly more challenging than the MM1 problem due to the inherent non-smoothness with CRN (see Figure 9). Therefore, it is highly probable that the majority of incumbent sequences converges to local optima, regardless of the solvers used.

We conducted tests on 20 instances of the SCONT problem, with varied parameters  $\mu_D = \{25, 50, 100, 200, 400\}$  and  $\mu_L = \{1, 3, 6, 9\}$ . In the majority of cases, ASTRO-BFDF demonstrated at least similar performance to ASTRO-DF, and sometimes surpassed it by uncovering superior solutions with a smaller budget. This success can be attributed to its ability to avoid getting trapped in local optima too quickly by leveraging the LF function. Detailed numerical results can be found in Appendix B.

## 6 Conclusion

This paper introduces ASTRO-BFDF, a novel stochastic TR algorithm tailored for addressing bi-fidelity simulation optimization. ASTRO-BFDF stands out for two key features: Firstly, it utilizes bi-fidelity Monte Carlo or crude Monte Carlo dynamically, adjusting sample sizes adaptively for both fidelity oracles within BAS. This ensures accurate estimation of function values, with the accuracy required for both function and gradient determined by the progress of optimization. Secondly, it strategically guides incumbents towards the neighborhood of the stationary point of the HF function by solely utilizing the LF function. These two features allow to achieve a faster convergence with enhanced computational efficiency, as demonstrated on several problems

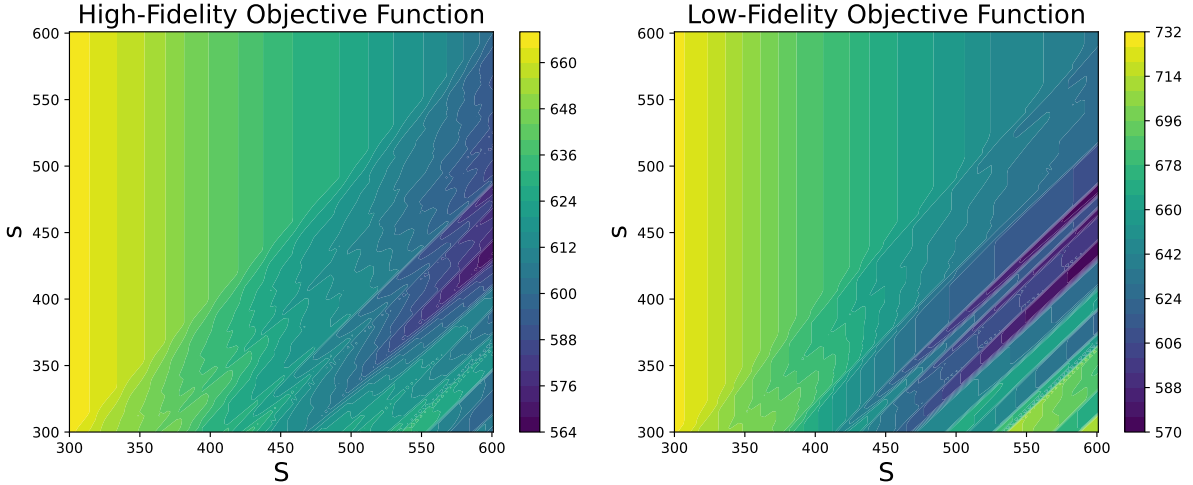


FIGURE 9: The contour maps of the HF and LF function of the SSSCONT problem with CRN. The HF simulator operates for 100 days, while the LF simulator runs for 30 days, indicating a cost ratio of 1:0.3.

including the synthetic problems and toy problems with DES. We also demonstrate the asymptotic behavior of the incumbents generated by ASTRO-BFDF, which converges to the stationary point almost surely.

## Acknowledgments

This work was authored by the National Renewable Energy Laboratory, operated by Alliance for Sustainable Energy, LLC, for the U.S. Department of Energy (DOE) under Contract No. DE-AC36-08GO28308. Funding for the algorithmic development and numerical experiment work was provided by Laboratory Directed Research and Development investments. Funding for the theoretical work (proofs) was provided by the Office of Science, Office of Advanced Scientific Computing Research, Scientific Discovery through Advanced Computing (SciDAC) program through the FASTMath Institute. The views expressed in the article do not necessarily represent the views of the DOE or the U.S. Government. The U.S. Government retains and the publisher, by accepting the article for publication, acknowledges that the U.S. Government retains a nonexclusive, paid-up, irrevocable, worldwide license to publish or reproduce the published form of this work, or allow others to do so, for U.S. Government purposes.

## A Proof of Lemma 5

*Proof.* Let us begin by noting that we have established from Step 13 in Algorithm 2 and Step 18 in Algorithm 3 that  $\Delta_k^h \geq \Delta_k^l$  almost surely for any  $k \in \mathbb{N}$ . Hence, if  $\Delta_k^h$  converges to zero almost surely, so does  $\Delta_k^l$ . Let us define the following index sets,

$$\begin{aligned}\mathcal{H} &:= \{k \in \mathbb{N} : (\hat{\rho}_k > \eta) \cap (\mu \|\nabla M_k^h(\mathbf{X}_k^0)\| \geq \Delta_k^h) \cap (I_k^h \text{ is True})\}, \\ \mathcal{L} &:= \{k \in \mathbb{N} : I_k^h \text{ is False}\}.\end{aligned}$$

We have, for any  $k \in \mathcal{H}$ ,

$$\begin{aligned}\tilde{F}(\mathbf{X}_k^0) - \tilde{F}(\mathbf{X}_k^s) &\geq \eta[M_k^h(\mathbf{X}_k^0) - M_k^h(\mathbf{X}_k^s)] \\ &\geq \frac{1}{2}\eta\kappa_{fcd}\|\nabla M_k^h(\mathbf{X}_k)\| \min\left\{\frac{\|\nabla M_k^h(\mathbf{X}_k)\|}{\|\mathbf{H}_k\|}, \Delta_k^h\right\} \\ &> \kappa_R(\Delta_k^h)^2,\end{aligned}\tag{28}$$

where  $\kappa_R := \min\{\eta\kappa_{fcd}(2\mu)^{-1} \min\{(\mu\kappa_{\mathbf{H}}^h)^{-1}, 1\}, \zeta\}$ . Note that (28) holds regardless of whether  $\mathbf{X}_k^s$  comes from minimizing  $M_k^l$  or  $M_k^h$ . We also obtain from Step 11 in Algorithm 3 that  $\tilde{F}(\mathbf{X}_k^0) - \tilde{F}(\mathbf{X}_k^s) \geq \zeta(\Delta_k^h)^2 \geq \kappa_R(\Delta_k^h)^2$  for any  $k \in \mathcal{L}$ . Hence, for any  $k \in \mathcal{K} := \mathcal{H} \cup \mathcal{L}$ ,

$$\kappa_R \sum_{k \in \mathcal{K}} (\Delta_k^h)^2 \leq \sum_{k \in \mathcal{K}} (f^h(\mathbf{X}_k) - f^h(\mathbf{X}_{k+1}) + \tilde{E}_k^0 - \tilde{E}_k^s) \leq f^h(\mathbf{x}_0) - f_*^h + \sum_{k=0}^{\infty} |\tilde{E}_k^0 - \tilde{E}_k^s|,$$

where  $f_*^h$  is the optimal value of  $f^h$ . We note that  $\mathcal{H}$  and  $\mathcal{L}$  are disjoint sets and for any  $k \notin \mathcal{K}$ ,  $\Delta_{k+1}^h = \gamma_2 \Delta_k^h$ . Let  $\mathcal{K} = \{k_1, k_2, \dots\}$ ,  $k_0 = -1$ , and  $\Delta_{-1}^h = \Delta_0^h/\gamma_2$ . Then from the fact that  $\Delta_k^h \leq \gamma_1 \gamma_2^{k-k_i-1} \Delta_{k_i}^h$  for  $k = k_i + 1, \dots, k_{i+1}$  and each  $i$ , we obtain

$$\sum_{k=k_i+1}^{k_{i+1}} (\Delta_k^h)^2 \leq \gamma_1^2 (\Delta_{k_i}^h)^2 \sum_{k=k_i+1}^{k_{i+1}} \gamma_2^{2(k-k_i-1)} \leq \gamma_1^2 (\Delta_{k_i}^h)^2 \sum_{k=0}^{\infty} \gamma_2^{2k} = \frac{\gamma_1^2}{1-\gamma_2^2} (\Delta_{k_i}^h)^2.$$

By Lemma 1, there must exist a sufficiently large  $K_{\Delta}$  such that  $|\tilde{E}_k^0 - \tilde{E}_k^s| < c_{\Delta}(\Delta_k^h)^2$  for any given  $c_{\Delta} > 0$  and any  $k \geq K_{\Delta}$ . Then, we have

$$\begin{aligned}\sum_{k=0}^{\infty} (\Delta_k^h)^2 &\leq \frac{\gamma_1^2}{1-\gamma_2^2} \sum_{i=0}^{\infty} (\Delta_{k_i}^h)^2 < \frac{\gamma_1^2}{1-\gamma_2^2} \left( \frac{(\Delta_0^h)^2}{\gamma_2^2} + \frac{f^h(\mathbf{x}_0) - f_*^h + E'_{0,\infty}}{\kappa_R} \right) \\ &< \frac{\gamma_1^2}{1-\gamma_2^2} \left( \frac{(\Delta_0^h)^2}{\gamma_2^2} + \frac{f^h(\mathbf{x}_0) - f_*^h + E'_{0,K_{\Delta}-1} + E'_{K_{\Delta},\infty}}{\kappa_R} \right),\end{aligned}$$

where  $E'_{i,j} = \sum_{k=i}^j |\tilde{E}_k^0 - \tilde{E}_k^s|$ . Then we get from  $E'_{K_{\Delta},\infty} < c_{\Delta} \sum_{K_{\Delta}}^{\infty} (\Delta_k^h)^2$  that

$$\sum_{k=K_{\Delta}}^{\infty} (\Delta_k^h)^2 < \frac{\gamma_1^2}{1-\gamma_2^2} \left( \frac{(\Delta_0^h)^2}{\gamma_2^2} + \frac{f^h(\mathbf{x}_0) - f_*^h + E'_{0,K_{\Delta}-1}}{\kappa_R} \right) \left( 1 - \frac{\gamma_1^2}{1-\gamma_2^2} \frac{c_{\Delta}}{\kappa_R} \right)^{-1}$$

Therefore,  $\Delta_k^h \xrightarrow{w.p.1} 0$  as  $k \rightarrow \infty$  and the statement of the theorem holds.  $\square$

## B Numerical Results (SSCONT)

In this section, we show the performance of ASTRO-DF and ASTRO-BFDF on 20 instances of the SCONT problem.  $\mu$  is the parameter for the demand and  $\theta$  is the parameter for Lead times. See Figure 10.

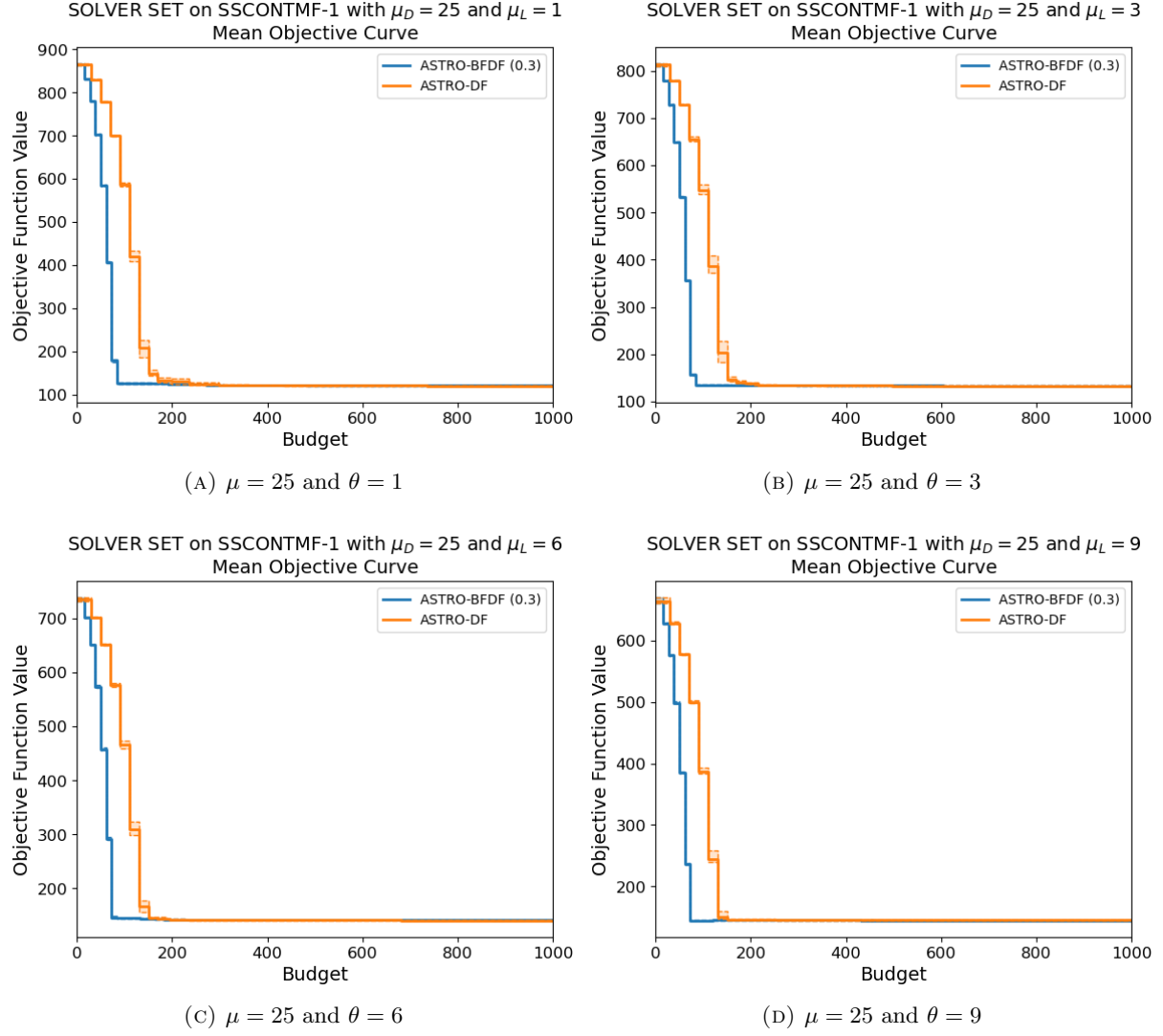


FIGURE 10: Optimization progress with 95% confidence intervals from 10 runs of ASTRO-DF and ASTRO-BFDF on SCONT.

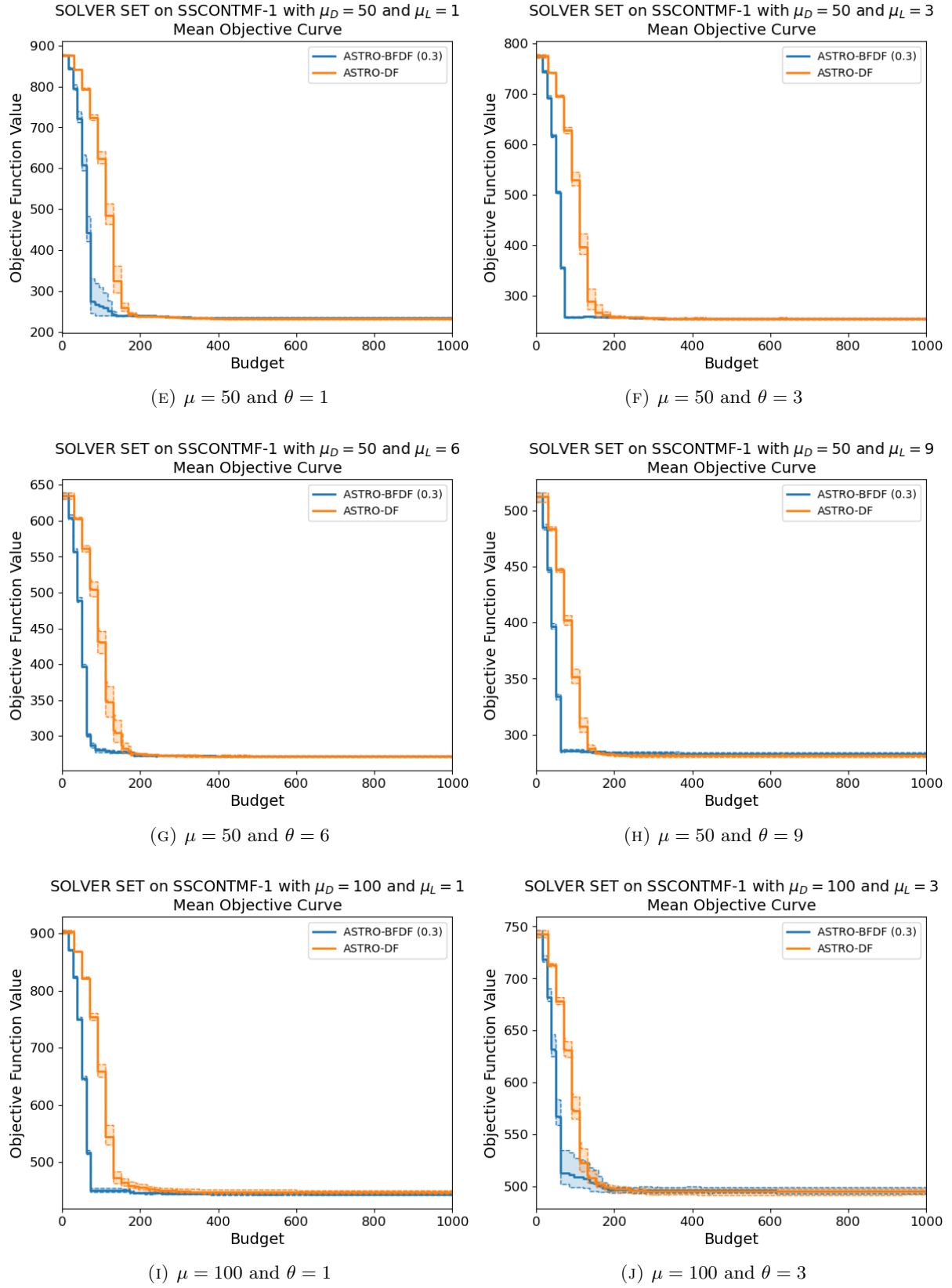


FIGURE 10: Optimization progress with 95% confidence intervals from 10 runs of ASTRO-DF and ASTRO-BFDF on SCONT.

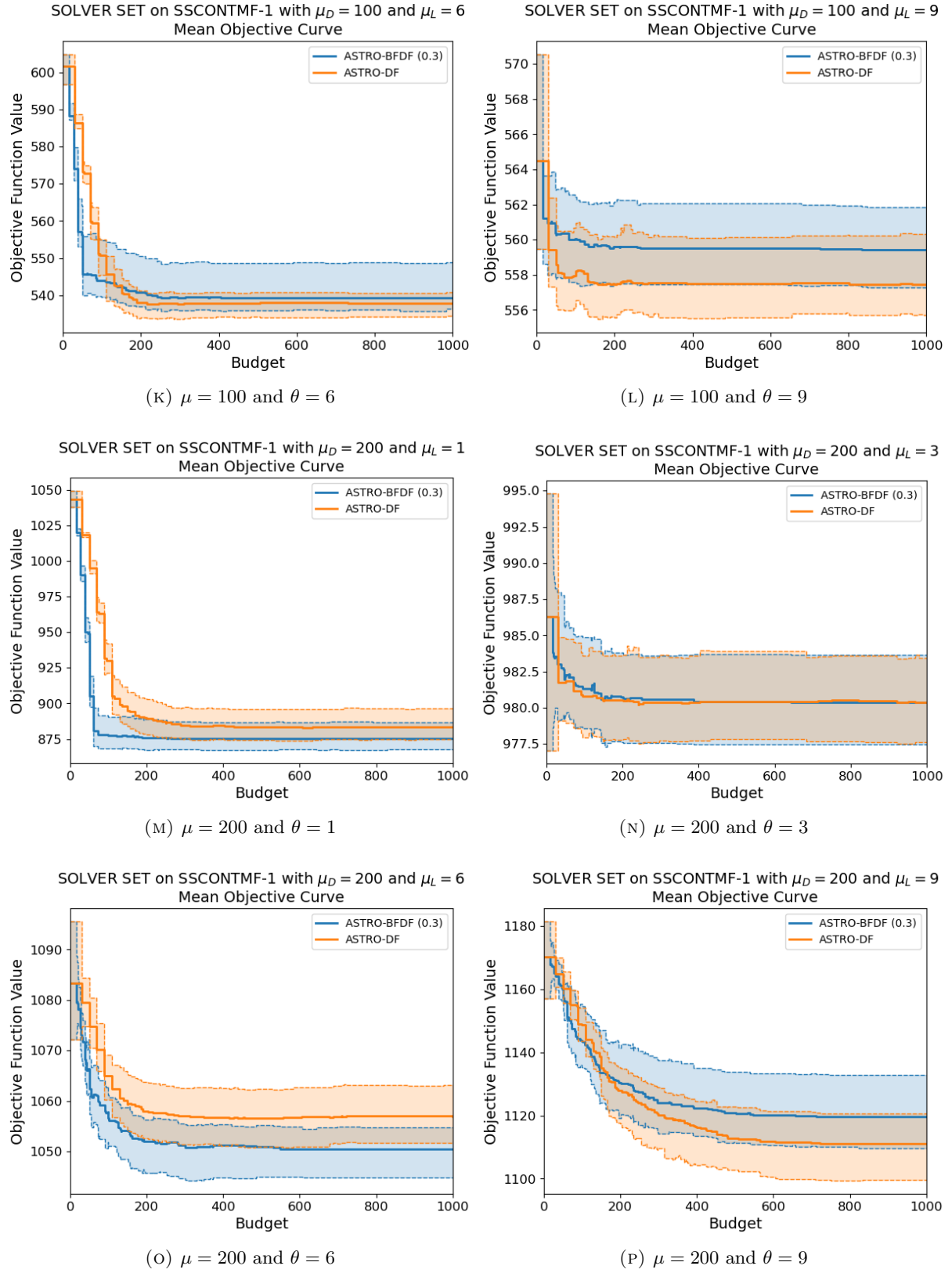


FIGURE 10: Optimization progress with 95% confidence intervals from 10 runs of ASTRO-DF and ASTRO-BFDF on SSCONT.

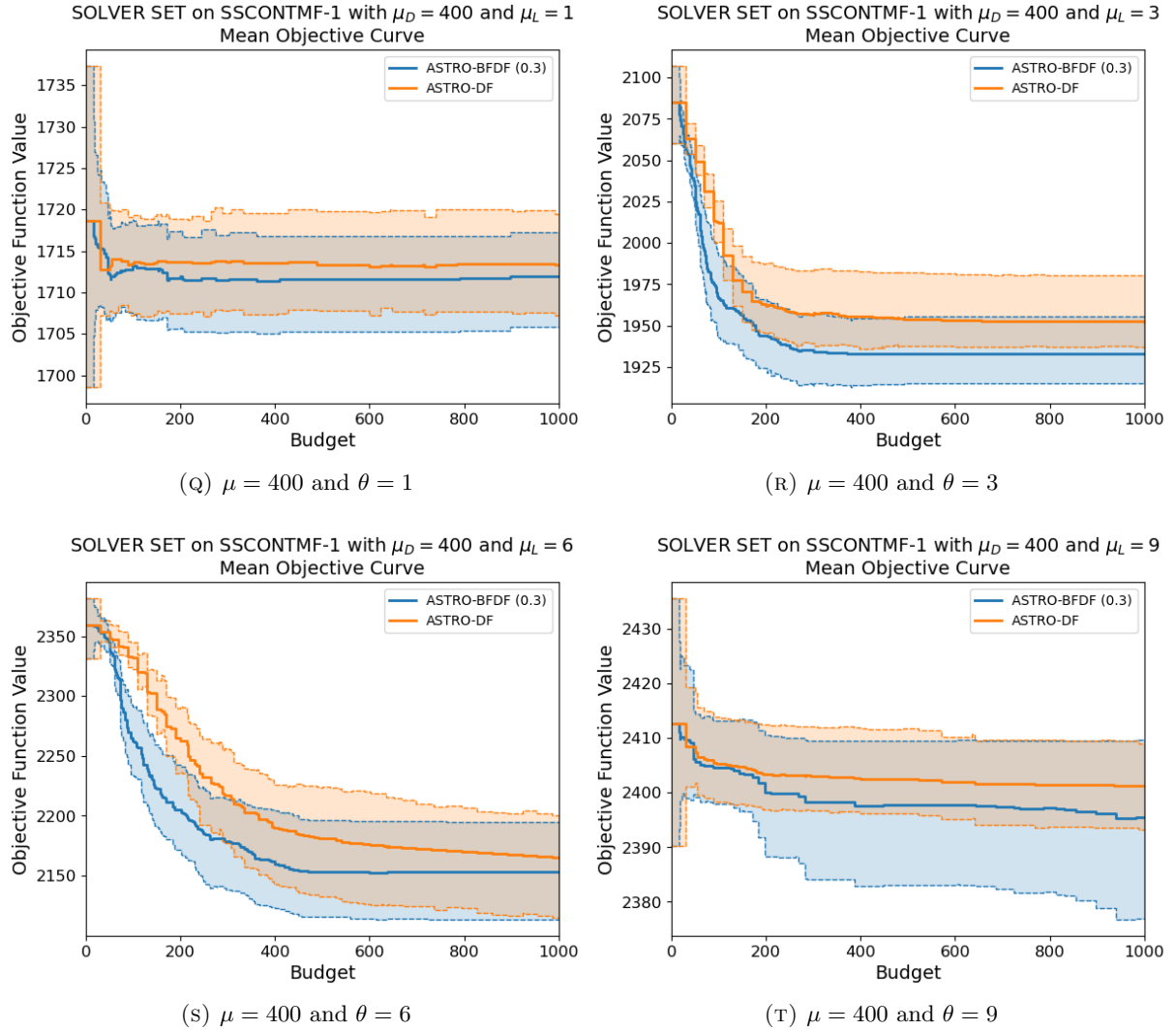


FIGURE 10: Optimization progress with 95% confidence intervals from 10 runs of ASTRO-DF and ASTRO-BFDF on SSCONT.

## C Implementation Details

All methods used the same parameters (e.g., TR radius  $\Delta_k$ , success ratio  $\eta_1$ ) where possible. ADAM and Nelder-Mead have used the default setting outlined in SimOpt github [14]. In terms of the design set selection for the model construction, ASTRO-DF has used  $2d+1$  design points with the rotated coordinate basis (See history-informed ASTRO-DF [22]). In the bi-fidelity scenario, we have employed two distinct design sets ( $\mathcal{X}_k$  and  $\mathcal{X}_k^l$ ) at Step 4 in Algorithm 2 and Step 6 in Algorithm 3 respectively.  $\mathcal{X}_k$  is selected to construct the local model for the HF function, implying that the computational costs for estimating the function value at  $\mathcal{X}_k$  is relatively high. Hence, the design set will be selected by reusing the design points within the TR and the corresponding replications as much as possible. To achieve this, we first pick  $d+1$  design points to obtain sufficiently affinely independent points by employing Algorithm 4.2 in [23]. After that, we pick additional  $d$  design points following the opposite direction to construct the quadratic interpolation

model with diagonal Hessian.  $\mathcal{X}_k^l$  consists of  $2d + 1$  design points, selected using the coordinate basis to minimize deterministic error owing to the lower cost of the LF oracle. In this scenario, the design set  $\mathcal{X}_k^l$  is optimally designed for design sets of any size ranging from  $d + 2$  to  $2d + 1$  (see [24]).

Hyper-parameters	ASTRO-BFDF
$\Delta_{\max}$ (maximum TR radius)	problem dependent
$\Delta_0^l$ and $\Delta_0^h$ (initial TR radius)	$10^{\lceil \log(\Delta_{\max}^2) - 1 \rceil / d}$
$\gamma_2$ (expansion constant)	1.5
$\gamma_1$ (shrinkage constant)	0.75
$\lambda_k$ (sample size lower bound)	5
$\kappa$ (adaptive sampling constant)	$F(\mathbf{X}_0) / (\Delta_0^h)^2$
$\eta$ (model fitness threshold)	0.1
$\alpha_0$ (initial correlation constant)	0.5
$\hat{\epsilon}$ (model gradient threshold)	0.001
$\zeta$ (sufficient reduction constant)	0.01

TABLE 1: Hyper-parameters for ASTRO-BFDF.

## References

- [1] A. S. Berahas, L. Cao, K. Choromanski, and K. Scheinberg, “A theoretical and empirical comparison of gradient approximations in derivative-free optimization,” *Foundations of Computational Mathematics*, vol. 22, no. 2, pp. 507–560, 2022.
- [2] R. Chen, M. Menickelly, and K. Scheinberg, “Stochastic optimization using a trust-region method and random models,” *Mathematical Programming*, vol. 169, no. 2, pp. 447–487, 2018.
- [3] K.-H. Chang, L. J. Hong, and H. Wan, “Stochastic trust-region response-surface method (strong)—a new response-surface framework for simulation optimization,” *INFORMS Journal on Computing*, vol. 25, no. 2, pp. 230–243, 2013.
- [4] Y. Ha and S. Shashaani, “Iteration complexity and finite-time efficiency of adaptive sampling trust-region methods for stochastic derivative-free optimization,” *arXiv:2305.10650*, 2023.
- [5] S. Ghadimi and G. Lan, “Stochastic first- and zeroth-order methods for nonconvex stochastic programming,” *SIAM Journal on Optimization*, vol. 23, no. 4, pp. 2341–2368, 2013.
- [6] L. W. Ng and K. E. Willcox, “Multifidelity approaches for optimization under uncertainty,” *International Journal for numerical methods in Engineering*, vol. 100, no. 10, pp. 746–772, 2014.
- [7] B. Peherstorfer, K. Willcox, and M. Gunzburger, “Survey of multifidelity methods in uncertainty propagation, inference, and optimization,” *Siam Review*, vol. 60, no. 3, pp. 550–591, 2018.
- [8] s. Xu, s. Zhang, s. Huang, s.-H. Chen, s. H. Lee, and s. Celik, “Efficient multi-fidelity simulation optimization,” in *Proceedings of the Winter Simulation Conference 2014*, pp. 3940–3951, IEEE, 2014.
- [9] S. De, K. Maute, and A. Doostan, “Bi-fidelity stochastic gradient descent for structural optimization under uncertainty,” *Computational Mechanics*, vol. 66, pp. 745–771, 2020.
- [10] R. Bollapragada, R. Byrd, and J. Nocedal, “Adaptive sampling strategies for stochastic optimization,” *SIAM Journal on Optimization*, vol. 28, no. 4, pp. 3312–3343, 2018.
- [11] S. Shashaani, F. S Hashemi, and R. Pasupathy, “ASTRO-DF: A class of adaptive sampling trust-region algorithms for derivative-free stochastic optimization,” *SIAM Journal on Optimization*, vol. 28, no. 4, pp. 3145–3176, 2018.
- [12] R. Bollapragada, C. Karamanli, and S. M. Wild, “Derivative-free optimization via adaptive sampling strategies,” *arXiv preprint arXiv:2404.11893*, 2024.

- [13] B. Peherstorfer, K. Willcox, and M. Gunzburger, “Optimal model management for multifidelity monte carlo estimation,” *SIAM Journal on Scientific Computing*, vol. 38, no. 5, pp. A3163–A3194, 2016.
- [14] D. J. Eckman, S. G. Henderson, S. Shashaani, and R. Pasupathy, “SimOpt.” <https://github.com/simopt-admin/simopt>, 2023.
- [15] Y. Ha, S. Shashaani, and R. Pasupathy, “Complexity of zeroth-and first-order stochastic trust-region algorithms,” *arXiv preprint arXiv:2405.20116*, 2024.
- [16] J. Müller, “An algorithmic framework for the optimization of computationally expensive bi-fidelity black-box problems,” *INFOR: Information Systems and Operational Research*, vol. 58, no. 2, pp. 264–289, 2020.
- [17] X. Song, L. Lv, W. Sun, and J. Zhang, “A radial basis function-based multi-fidelity surrogate model: exploring correlation between high-fidelity and low-fidelity models,” *Structural and Multidisciplinary Optimization*, vol. 60, pp. 965–981, 2019.
- [18] D. J. Eckman, S. G. Henderson, and S. Shashaani, “Diagnostic tools for evaluating and comparing simulation-optimization algorithms,” *INFORMS Journal on Computing*, vol. 35, no. 2, pp. 350–367, 2023.
- [19] D. P. Kingma and J. Ba, “Adam: A method for stochastic optimization,” 2017.
- [20] R. R. Barton and J. S. Ivey Jr, “Nelder-mead simplex modifications for simulation optimization,” *Management Science*, vol. 42, no. 7, pp. 954–973, 1996.
- [21] L. Mainini, A. Serani, M. P. Rumpfkeil, E. Minisci, D. Quagliarella, H. Pehlivan, S. Yildiz, S. Ficini, R. Pellegrini, F. Di Fiore, *et al.*, “Analytical benchmark problems for multifidelity optimization methods,” *arXiv preprint arXiv:2204.07867*, 2022.
- [22] Y. Ha and S. Shashaani, “Towards greener stochastic derivative-free optimization with trust regions and adaptive sampling,” in *2023 Winter Simulation Conference (WSC)*, pp. 3508–3519, IEEE, 2023.
- [23] S. M. Wild, R. G. Regis, and C. A. Shoemaker, “Orbit: Optimization by radial basis function interpolation in trust-regions,” *SIAM Journal on Scientific Computing*, vol. 30, no. 6, pp. 3197–3219, 2008.
- [24] T. M. Ragonneau and Z. Zhang, “An optimal interpolation set for model-based derivative-free optimization methods,” *arXiv preprint arXiv:2302.09992*, 2023.